

1 **Thermal processes of thermokarst lakes in the continuous**
2 **permafrost zone of northern Siberia - observations and**
3 **modeling (Lena River Delta, Siberia)**

4

5 **J. Boike¹, C. Georgi¹, G. Kirilin², S. Muster¹, K. Abramova³, I. Fedorova^{4,5,6}, A.**
6 **Chetverova^{4,5}, M. Grigoriev,⁷ N. Bornemann¹ and M. Langer^{1,8}**

7 [1] Alfred Wegener Institute Helmholtz Center for Polar and Marine Research,
8 Telegrafenberg A43, 14473 Potsdam, Germany

9 [2] Leibniz-Institute of Freshwater Ecology and Inland Fisheries (IGB), Mueggelseedamm
10 310, 12587 Berlin, Germany

11 [3] Lena Delta Nature Reserve, Ak. Fedorova 28, 678400 Tiksi, Sakha Republic, Russia

12 [4] Institute of Earth Science, Saint-Petersburg State University, 10th line of Vasiljevsky
13 Island, 33-35. 199178 Saint-Petersburg, Russia

14 [5] Arctic and Antarctic Research Institute, 38, Beringa str., St. Petersburg, 199397, Russia

15 [6] Kazan Federal University, 18, Kremlyovskaya str., Kazan, Russia

16 [7] Melnikov Permafrost Institute, Siberian Branch, Russian Academy of Sciences, Yakutsk,
17 Russia

18 [8] Laboratoire de Glaciologie et Géophysique de l'Environnement (LGGE), 38402 St Martin
19 d'Hères Cedex, France

20

21 Correspondence to: J. Boike (Julia.Boike@awi.de)

1 **Abstract**

2 Thermokarst lakes are typical features of the northern permafrost ecosystems, and play an
3 important role in the thermal exchange between atmosphere and subsurface. The objective of
4 this study is to describe the main thermal processes of the lakes and to quantify the heat
5 exchange with the underlying sediments. The thermal regimes of five lakes located within the
6 continuous permafrost zone of northern Siberia (Lena River Delta) were investigated using
7 hourly water temperature and water level records covering a three year period (2009-2012),
8 together with bathymetric survey data. The lakes included thermokarst lakes located on
9 Holocene river terraces that may be connected to Lena River water during spring flooding,
10 and a thermokarst lake located on deposits of the Pleistocene Ice Complex. Lakes were
11 covered by ice up to 2 m thick that persisted for more than 7 months of the year, from October
12 until about mid-June. Lake-bottom temperatures increased at the start of the ice-covered
13 period due to upward-directed heat flux from the underlying thawed sediment. Prior to ice
14 break-up, solar radiation effectively warmed the water beneath the ice cover and induced
15 convective mixing. Ice break-up started at the beginning of June and lasted until the middle or
16 end of June. Mixing occurred within the entire water column from the start of ice break-up
17 and continued during the ice-free periods, as confirmed by the Wedderburn numbers, a
18 quantitative measure of the balance between wind mixing and stratification that is important
19 for describing the biogeochemical cycles of lakes. The lake thermal regime was modelled
20 numerically using the FLake model. The model demonstrated good agreement with
21 observations with regard to the mean lake temperature, with a good reproduction of the
22 summer stratification during the ice free period, but poor agreement during the ice covered
23 period. Model sensitivity to lake depth demonstrated that lakes in this climatic zone with
24 mean depths >5 m develop continuous stratification in summer for at least one month. The
25 modeled vertical heat flux across the bottom sediment tends towards an annual mean of zero,
26 with maximum downward fluxes of about 5 W m^{-2} in summer and with heat released back
27 into the water column at a rate of less than 1 W m^{-2} during the ice-covered period.

28 The lakes are shown to be efficient heat absorbers and effectively distribute the heat through
29 mixing. Monthly bottom water temperatures during the ice-free period range up to 15°C and
30 are therefore higher than the associated monthly air or ground temperatures in the surrounding
31 frozen permafrost landscape. The investigated lakes remain unfrozen at depth, with mean
32 annual lake –bottom temperatures of between 2.7 and 4°C .

- 1 The data are available in the supplementary material for this paper and through the
- 2 PANGAEA website (<http://doi.pangaea.de/10.1594/PANGAEA.846525>).

1 **1 Introduction**

2 Lakes can be interpreted as sensitive climatic indicators that respond to a range of different
3 influences affecting the world's climate. They can also exert an important influence on the
4 local, regional, and global climate and hydrology by regulating heat and water fluxes, but
5 their thermal dynamic represented in RCMs and GCMs is rather simple, and does not include
6 all physical processes that are necessary for reproducing atmosphere-lake interaction (Walsh
7 et al., 1998; Martynov et al., 2012). Lakes are often typical features of northern hemisphere
8 ecosystems (Figure 1). In permafrost areas, which occupy about 25% of the world's landmass,
9 lakes influence not only the thermal regime of the surrounding and underlying permafrost, but
10 also the atmospheric heat and water fluxes, due to their large thermal heat reservoirs and heat
11 capacities. The winter heat flux into the atmosphere through the ice cover from deep lakes
12 that remain unfrozen at depth is several times greater than that from the surrounding tundra
13 (Jeffries et al., 1999). Even smaller polygonal water bodies (thermokarst ponds), which freeze
14 to the bottom every winter, have heat fluxes that are an order of magnitude greater than those
15 from the surrounding permafrost (Langer et al., 2011b). The large thermal heat reservoir in
16 lakes prevents the sediment beneath those lakes with a water depth greater than about 2 or 3
17 meters from freezing, thus allowing a talik to develop (Lachenbruch, 1962). However, little
18 data exists on the thermal conditions of lakes in north and central Yakutia, or the taliks
19 beneath them (Grigoriev, 1960, 1966; Are, 1974; Pavlov et al., 1981). These unfrozen layers
20 of lake sediment can enhance mobilization of the carbon reservoir by enabling year-round
21 microbial decomposition in otherwise frozen surroundings, and water bodies can thus be
22 hotspots for CO₂ and CH₄ emissions (Langer et al., 2015; Schneider von Deimling et al.,
23 2014; Walter et al., 2006; Abnizova et al., 2012; Laurion et al., 2010). Water bodies are also
24 important because they provide habitats for zooplankton, fish, and migratory birds (Vincent
25 and Hobbie, 2000; Alerstam et al., 2001), and are a source of drinking water for northern
26 communities, of water for irrigation, and of water for industry, exploration, and ice-road
27 construction in winter (Vincent et al., 2013).

28 Measuring the water temperatures in lakes over both short and long terms is therefore
29 important, not only for modeling the development of the subsurface thermal regime, but also
30 for understanding and modeling ecological and physical dynamics. Few investigations have,
31 however, been carried out into the physical and thermal characteristics of Arctic water bodies,
32 especially over the long term, and there is a particular shortage of data from northern Siberia.

1 A notable exception is the long term biological, physical and chemical lake study initiated in
2 1975 at the Toolik Lake Long Term Ecological Research (LTER) site in Alaska. The lakes
3 studied are located on the North Slope of Alaska, in the foothills of the Brooks Range, and are
4 classified as low Arctic lakes (Hobbie and Kling, 2014). Toolik Lake and most of the other
5 lakes in this area are “kettle lakes” that formed as a result of glaciation; their lake
6 morphometries (surface areas, depths) are a result of the glaciation history and the age of the
7 landscape. Water depths can range up to 25 m, as is the case in Toolik Lake (Hobbie and
8 Kling, 2014). The thermal stratification varies considerably between lakes (depending on the
9 lake’s morphometry), as well as between years (Luecke et al., 2014). Also in northern Alaska,
10 Arp et al. (2010) made use of an original method that combined short term (for example, over
11 one year) measured lake surface temperatures (from depths of 0.5 m and 1.0 m) with
12 meteorological and remote sensing data on lake surface temperatures and ice thicknesses. The
13 latter variables were compared with measured temperatures and ice thicknesses, and with
14 modeled results (Arp et al., 2010). The advantage of this approach is that, following
15 successful calibration, a monitoring network can be established that is based purely on remote
16 sensing data. Monitoring in some of these lakes on the Alaskan Coastal Plain has continued
17 since 2010 as part of the new Circum-Arctic Lakes Observation Network (CALON) initiative
18 (<http://www.arcticlakes.org/calon-lakes.html>; Hinkel et al., 2012). An initial series of data for
19 vertical temperature profiles from the summer of 2010 has been provided for a number of
20 lakes, together with time series of hourly temperature data, in order to demonstrate the
21 seasonal and temporal variability (Hinkel et al., 2012).

22 Sporadic measurements of lake temperatures have been obtained in conjunction with
23 limnological studies (for example, by Keatley et al., 2007, or Pienitz et al., 1997),
24 paleolimnological investigations (such as in the 172 m deep El’gygytyn Lake of north-
25 eastern Siberia, a meteoritic impact crater; Nolan and Brigham-Grette, 2006), and physical
26 experiments (such as dye tracing under the ice cover in a small Arctic lake; Welch and
27 Bergmann, 1985). Vincent et al. (2008) measured temperatures and salinity in a high Arctic,
28 125 m deep, perennially ice-covered lake on Ellesmere Island in Nunavut, Canada. The
29 authors then successfully modeled the lake’s temperature regime using a one-dimensional
30 heat diffusion equation and including heat transfer by radiation through ice and water. For
31 lakes within the Mackenzie Delta (Northwest Territories of Canada), Burn (2002, 2005)
32 demonstrated that the temperatures in the deep central pool of a thermokarst lake on Richards
33 Island remained positive throughout the winter, with a mean annual temperature of 3.5°C,

1 whereas freezing occurred in the shallow littoral terrace of the lake (mean annual temperature
2 -3.7°C).

3 This paper aims to quantify the seasonal thermal dynamics of lakes in the Eurasian north,
4 where monitoring observatories have recently been established in the central part of the Lena
5 River Delta. Our objectives are (i) to describe the thermal patterns and processes in both
6 thermokarst lakes and “perched” lakes (which can have seasonal connections to river water),
7 and (ii) to make use of measured data to validate the freshwater model FLake, as well as
8 estimate water sediment heat exchange. FLake offers a good compromise between
9 computational efficiency and physical reality, and has been coupled to several regional and
10 global climate models (Thiery et al., 2014; Martynov et al., 2010). FLake has been
11 used in various 1 dimensional modeling studies, for a wide range of lakes, including tropical
12 lakes, and in lake model intercomparison projects (LakeMIP; Thiery et al., 2014; Stepanenko
13 et al., 2010). However, it has not been used for Arctic lakes and this study tests the ability of
14 FLake to reproduce the temperature regimes of thermokarst lakes in northern Siberia.

15

16

17 **2 Site description**

18 The Lena River Delta in northern Yakutia is one of the largest deltas in the Arctic and has one
19 of the largest catchment areas ($2,430,000\text{ km}^2$) in the whole of Eurasia (Costard and Gautier,
20 2007). The Lena River discharges about 525 km^3 of water through the delta into the Arctic
21 Ocean every year, with an average annual discharge rate of $16,800\text{ m}^3\text{ s}^{-1}$ (Gordeev and
22 Sidorov, 1993). This discharge rate has been reported to be increasing (Fedorova et al., 2015;
23 Rawlins et al., 2009). As it passes through its estuarine area, the main flow of the Lena River
24 splits into numerous arms and transverse branches to form the most extensive delta in the
25 Russian Arctic, covering $25,000\text{ km}^2$ and including about 1,500 islands and 60,000 lakes.

26 Continuous cold permafrost (with a mean annual temperature of -10°C at 10 m depth)
27 underlies the study area to between about 400 and 600 m below the surface. Since
28 observations started in 2006, the permafrost at 10.7 m depth has warmed by $> 1.5^{\circ}\text{C}$ (Boike et
29 al., 2013; <http://gtnpdatabase.org/boreholes/view/53/>).

30 The main features of the annual energy balance for these sites with continuous permafrost in
31 the subsurface typically include low net radiation, higher atmospheric latent heat flux than

1 sensible heat flux, and a large proportion of soil heat flux (Boike et al., 2008; Langer et al.,
2 2011a, 2011b). Previous publications have reported that shallow (< 1 m deep) ponds freeze
3 completely in winter, but that the timing of freeze-back can vary by up to 2 months between
4 years, depending on the surface energy balance (Langer et al., 2011b; Langer et al., 2015).

5 The study areas are located on the islands of Samoylov and Kurungnakh, within the central
6 part of the Lena River Delta (Figure 1). Samoylov Island (72°22'N, 126°28'E) lies within one
7 of the main river channels in the southern part of the delta and is relatively young, with an age
8 of between 4 and 2 ka BP (Schwamborn et al., 2002), which is also the estimated maximum
9 age of the investigated lakes on the island. In contrast, Kurungnakh Island forms part of the
10 third terrace of the Lena Delta and is an erosional remnant of a late-Pleistocene accumulation
11 plain. It consists of fluvial sands overlain by Yedoma-type ice complex deposits, which
12 accumulated between 100 and 50 ka BP and since 50 ka BP, respectively, and a Holocene
13 cover (8 to 3 ka BP) (Schwamborn et al., 2002; Wetterich et al., 2008). Large thermokarst
14 lakes and basins are major components of the ice-rich permafrost landscape of Kurungnakh
15 Island; they have formed since 13 to 12 ka BP (Morgenstern et al., 2011, 2013).

16 The lakes presented in this paper are of thermokarst origin which is common for the lowland
17 tundra permafrost areas of North East Siberia. These areas were not ice-covered during the
18 latest glacial period (70,000-10,000 years ago) and are characterized by high to moderate
19 ground ice content and thick sediment cover. Arctic lowlands with similar landscape
20 characteristics and lake distributions can be found in Central and East Siberia, Interior and
21 Northern Alaska as well as Northwest Canada (Grosse et al., 2013).

22 The landscape on both of these islands, and in the delta as a whole, has generally been shaped
23 by water through erosion and sedimentation (Fedorova et al., 2015), and by thermokarst
24 processes (Morgenstern et al., 2013). The proportion of the total land surface of the delta
25 covered by surface water can amount to more than 25% (Muster et al., 2012). Up to 50% of
26 the total surface water area in permafrost landscapes is attributed to small lakes and ponds
27 with surface areas of less than 10^5 m², which have the potential to grow into large thermokarst
28 lakes (Muster et al., 2012). Water budget modeling for the tundra landscape has shown a
29 small positive balance since 1953, which has been confirmed by satellite observations (since
30 1964) of the surface areas of water bodies (Boike et al., 2013). The chemical and isotopic
31 signals from the water in lakes on Samoylov Island generally indicate low levels of
32 mineralization (Table 1). The stable isotopic ratios indicate that the thermokarst lake water is

1 sourced mainly from thawed ground ice mixed with precipitation and the water in shallow
2 ponds is sourced mainly from summer precipitation (Abnizova et al., 2012).

3 Small ponds and lakes emit more CO₂ and CH₄ per square meter than the surrounding tundra,
4 and greenhouse gas production continues during winter in those lakes that do not freeze to the
5 bottom (Langer et al., 2015). Modeling studies have demonstrated that an unfrozen layer of
6 lake sediment is maintained throughout the year beneath thermokarst lakes (Yi et al., 2014).
7 During high spring floods some of the lakes on the first terrace are flooded with Lena River
8 water. Observations in 2014 on Samoylov Island, for example, confirmed the flooding of a
9 large part of the first terrace on the island, including most of the lakes.

10 Additional detailed information concerning the climate, permafrost, land cover, vegetation,
11 and soil characteristics of these islands in the Lena River Delta can be found in Boike et al.
12 (2013) and Morgenstern et al. (2013).

13

14 **3 Methods**

15 **3.1 Field instrumentation and ground surveys**

16 In July 2009, water level and temperature sensors (HOBO Temp Pro v2, HOBO U20, Onset,
17 $\pm 0.2^\circ\text{C}$ across a temperature range from 0°C to 70°C , and $\pm 0.4^\circ\text{C}$ across a temperature range
18 from -40°C to 0°C) were installed within the water columns of the investigated lakes on
19 Samoylov and Kurungnakh Island. Figure 1 shows the locations of the lakes (labelled
20 Sa_Lake_1-4 for Samoylov and Ku_Lake_1 for Kurungnakh) and the location of the long
21 term weather station. Gaps in the climate data record (air temperature, radiation, humidity,
22 wind speed and direction, and snow depth) were filled whenever possible with data from
23 temporary climate and eddy covariance stations located in close proximity to the weather
24 station (Boike et al., 2013). Temperature and water depth sensors were placed directly above
25 the sediment-water interface and then temperature sensors at 2 m intervals up to 2 m below
26 the water surface (Figure 2). The sensors were suspended in the water column from a buoy
27 and anchored in the sediment below. The sensor at the bottom of the lake (just above the
28 sediment) was labelled as “0 m”, the sensor 2 m above the sediment as “2 m”, and so on. The
29 uppermost sensors were usually about 2 m below the water surface since we were concerned
30 about the formation of ice and the potential drift of sensors with the shifting of ice cover. End-
31 of-winter ice thickness (obtained by drilling) was measured in 2014; it ranged between 1.9

1 and 2 m in lakes Sa_Lake_1-4 on Samoylov Island. During some winters the uppermost
2 sensors became enclosed within the ice cover (for example, Sa_Lake_1 in 2012), but they
3 were not moved out of position. One sensor was installed in the Lena River during August
4 2009 (Figure 1) and recorded data from July 2009 to August 2010 but was lost during the
5 following year.

6 Sensors were usually retrieved once a year (in August) and then re-launched in approximately
7 the same position. The temperature record was therefore briefly interrupted during the period
8 when the sensors were retrieved and read. The water depth (“sensor depth”) recorded by the
9 bottom sensor sometimes changed following retrieval due to a change in the sensor position,
10 although the actual water level of the lake remained the same. For example, for Sa_Lake_4 (a
11 perched lake), sensors that were deployed at a water depth of about 8.5 m in 2009 were
12 reinstalled at a depth of about 9.5 m in August 2010. Water level variations due to water
13 balance changes (when the sensor position had not changed), for example during the summer
14 period, were usually less than 0.5 m.

15 Data is only available over a one-year period for the lake on Kurungnakh Island (2009-2010)
16 as the loggers were subsequently displaced, presumably during ice break-up. For the lakes on
17 Samoylov Island, however we obtained continuous temperature and water level data over a
18 period of 3 years from 2009 to 2012. All data and metadata are provided in the supplementary
19 material for this publication and through the PANGAEA website
20 (<http://doi.pangaea.de/10.1594/PANGAEA.846525>).

21 Bathymetric surveys were carried out in 2009 and 2010 on all of the investigated thermokarst
22 lakes, using a GPSMAP 178 C echo sounder, a GPSMAP 421S plotter and a GPS 60
23 navigator, all from Garmin. The shorelines were mapped either by GPS field survey or by
24 manually digitizing the shoreline from high resolution aerial images. The accuracy of the echo
25 sounder equipment was about 0.1 m and was regularly checked using manual profiling. Depth
26 measurements were taken along the longest lake axis as well as along a zigzag track in order
27 to cover most of the lake surface and to locate any local “holes” that might exist as a result of
28 thermokarst processes. Surface areas, mean and maximum depths, volumes, and hypsographic
29 (depth/area) curves were calculated for the five lakes investigated using linear distance
30 nearest neighbor interpolation in ArcGIS software (v.10.1) (Table 1). A description of the
31 morphometry, including two-dimensional contour plots and cross sectional profiles of the
32 lakes can be found in the appendix of this paper (Figures A1 to A5). Bathymetric records

1 were also obtained for eight additional lakes (Chetverova et al., 2013) but are not included
2 herein since temperature sensors were not installed. Bathymetric data, metadata and
3 morphometric descriptions can be found in the appendix material for this publication, as well
4 as through the PANGAEA website (<http://doi.pangaea.de/10.1594/PANGAEA.846525>).

5

6 **3.2 Heat content**

7 The ability of lakes to store and redistribute additional heat at seasonal time scales may affect
8 the heat budget of adjacent permafrost areas at the landscape spatial scale. For this reason, we
9 observe the thermal regime of tundra lakes to make inferences about their effect on heat
10 exchange processes. The heat content of each lake (H_l) was calculated at hourly time steps
11 from the thermal energy stored in a water column from the lake's surface to its maximum
12 depth (z_{\max}):

$$13 \quad H_l = c_w \rho_w \int_0^{z_{\max}} T(z, t) dz \quad (1)$$

14 where c_w is the specific heat capacity of water, ρ_w is the freshwater density, and T is the
15 temperature. The calculated heat budgets were divided into different time periods, as
16 proposed by Wetzel (2001). The summer heat income is defined as the amount of heat
17 required to raise the temperature of the lake from isothermal conditions at 4°C to the
18 maximum observed depth-averaged summer temperature (summer heat content). The winter
19 heat income is the amount of heat required to raise the temperature from the minimum
20 temperatures to 4°C. The annual heat budget is the total amount of heat necessary to raise the
21 water from the minimum temperature to maximum summer temperature. The winter heat
22 income and the annual heat budget must include the latent heat of fusion for the ice cover,
23 especially for high latitude lakes (Wetzel, 2001). The ice cover thickness was measured
24 during May 2014 and varied slightly from 2 m (Sa_Lake_1, Sa_Lake_2) to 1.9 m
25 (Sa_Lake_4). The ice cover in these lakes melts completely every summer so that freezing
26 and melting energies usually balance out over a year. The timing of spring ice break-up
27 extends from the first ice melt, through moat formation and drifting of the ice cover, to the
28 complete disappearance of ice. It is defined herein as the time at which the temperatures from
29 all sensors indicate isothermal conditions, with temperature differences from the bottom to the
30 top of the water column of < 0.1°C following the period of stratification that occurs during ice
31 cover, i.e. the time at which the lake water becomes completely mixed. The ice formation in

1 fall is defined by the start of stratification in lake temperatures, i.e. when temperature
2 differences from bottom to top exceed 0.1°C. The uncertainties in these determined times are
3 estimated to be +/- 5 days and are based on comparison with (infrequently available) satellite
4 data (Table 1).

5

6 **3.3 Modeling of lake thermodynamics**

7 FLake is a freshwater lake model (Mironov, 2005) aimed at predicting the vertical thermal
8 structure and mixing conditions in lakes over periods ranging from a few hours to a few years.
9 The model is based on a two-layer parametric representation of the evolving temperature
10 profile in the water column and on the integrated heat and kinetic energy budgets. The upper
11 mixed layer is treated as thermally homogeneous, while the structure of the stratified layer
12 between the upper mixed layer and the bottom of the basin (the lake thermocline) is described
13 using the concept of self-similarity (or assumed shape) of the temperature-depth curve. The
14 same self-similarity concept is used to describe the temperature structure of the thermally
15 active upper layer of bottom sediments (Golosov and Kirillin, 2010) and of the ice (Mironov
16 et al., 2012). It should be noted that no change in water depth as a result of winter ice
17 formation is included in the computation, and the water depth is therefore assumed to be
18 constant. Precipitation is also not included as an input into the model and snow accumulation
19 is therefore not computed. Visual observations confirm that the lakes are usually snow free
20 due to the generally low snowfall (although a few areas with snow and hardened wind crusts
21 occur locally), combined with high wind speeds blowing the snow away.

22 The following input data and settings were used for the lakes investigated in this study and
23 tested with data for Sa_Lake_1, i.e. a lake depth of 4 m (93% of this lake has a water depth of
24 not more than 4 m), a water optical light extinction coefficient of 0.5 m⁻¹, a 6 m thickness for
25 the thermally active sediment layer beneath the lake, and a temperature at the bottom of the
26 thermally active sediment layer of 4.5°C. Due to their very low contents of organic material
27 and low levels of biological productivity the lakes are usually very clear: in shallow lakes (for
28 example, Sa_Lake_3) the lake bottom is visible even at 2 m water depths. The thermal
29 characteristics of the sediment are based on sediment temperatures measured beneath two
30 lakes in the Lena River Delta (on the Bykovsky Peninsula; Grigoriev, 1993) and are discussed
31 in the Sects. 4 and 5. Two temperature profiles were obtained in June 1984 for one shallow (1

1 m) and one deep (5 m) lake, down to a sediment depth of 16 and 21 m below the lake bed,
2 respectively. These temperature profiles are used as input for the model experiments since the
3 assumption of thermal equilibrium does not necessarily exist for the lakes in the permafrost
4 landscape.

5 Two meteorological datasets were used to drive the model: (1) hourly data from the on-site
6 weather station (air temperature at 2 m height, wind speed, humidity, and radiation
7 components), and (2) 6-hourly NCEP/NCAR reanalysis data provided by the
8 NOAA/OAR/ESRL PSD, Boulder, Colorado, USA (<http://www.esrl.noaa.gov/psd/>; Kalnay
9 et al., 1996). The two driving datasets were compared and were found to be in good
10 agreement with each other, having some discrepancies in the short wave radiation
11 components (Figure 3). The modeled lake temperatures were nearly identical in both
12 datasets (not shown), indicating that reanalysis data sets perform well for lake modeling in
13 these remote areas, where on-site meteorological information is often limited. For further
14 analysis we used the measured on-site meteorological dataset, which can be found in the
15 supplementary material for this publication. The FLake model output parameters (water
16 temperatures, ice cover thickness, bottom sediment heat flux) for one of the lakes
17 (Sa_Lake_1) are compared for the time period 9 July 2009 to 29 July 2011 with the measured
18 parameters in Sect. 4. The model was used to:

- 19 - validate the 1-dimensional modeling approach and qualify of the main mechanisms
20 governing features of the lake thermal regime, such as summer stratification, water-sediment
21 heat exchange, and ice melt
- 22 - characterize the water-sediment heat exchange at annual time scales
- 23 - establish a relationship between the morphometry and summer stratification duration.

24 The “Lake Analyzer” numerical tool (<http://lakeanalyzer.gleon.org/>; Read et al., 2011) was
25 used to determine the dimensionless Wedderburn number (Wd), a quantitative measure of the
26 balance between wind mixing and stratification that is important for describing the
27 biogeochemical cycles of lakes (Spigel and Imberger 1980). A Wd number of 1 indicates a
28 threshold value at which the wind shear brings the thermocline to the lake's surface along the
29 upwind shoreline. For large Wedderburn numbers ($\gg 1$) the buoyancy force is much greater
30 than the wind stress suggesting strong vertical stratification. For small Wedderburn numbers
31 ($\ll 1$) the wind stress is much greater than the buoyancy force suggesting destruction of the
32 vertical thermal stratification in the lake. On-site weather data from hourly time series of

1 water temperature, wind speed, and bathymetric data were used as model inputs for the
2 calculation of W_d .

3

4

5 **4 Results**

6 **4.1 Lake thermal dynamics based on observations**

7 The following analyses were based on temperature and sensor depth (water depth) data
8 collected over the course of three years (2009-2012) from the investigated lakes, covering a
9 range of morphometric characteristics and located on two geomorphologically different
10 terraces (consisting of sediments of the Pleistocene Ice Complex on Kurungnakh and a
11 Holocene flood plain on Samoylov). The seasonal thermal dynamics are only discussed in
12 detail for two of these lakes: Sa_Lake_1 which is a thermokarst lake, and Sa_Lake_4 which is
13 a perched/oxbow lake (Figures 4 and 5; an animation of the daily temperatures of Sa_Lake_1
14 is also provided in the supplement). These lakes were selected as they have the best data
15 records, taking into account the temporal coverage and the total number of sensors in each
16 lake profile. The seasonal temperature dynamics of the other lakes (Sa_Lake_2, Sa_Lake_3,
17 and Ku_Lake_1) are illustrated in the Appendix of this paper (Figures A6-A8).

18 **4.2 Fall & winter**

19 During fall, cooling and complete mixing occurs at about the end of September resulting in
20 isothermal conditions at 0°C immediately prior to ice cover formation (Figures 4 & 5). The
21 ice cover growth can be briefly interrupted due to short-lived warming events during the fall
22 (as was observed, for example, in late September and early October of 2008) but the ice cover
23 then persists from October through to June (Figures 4b & 5c; Table 1). The water column
24 becomes stratified following the formation of the ice cover and the initial isothermal
25 conditions change so that lake-bottom temperatures are consistently warmer than those higher
26 up in the water column (towards the water/ice interface). This bottom temperature
27 development under ice, which involves rapid warming immediately after ice-cover formation
28 followed by subsequent gradual cooling, takes place in all lakes but the rates of warming and
29 cooling vary (Figures 4b, 5c, A6-8). In Sa_Lake_1 the maximum vertical temperature
30 gradient was less than 1°C m^{-1} (with a maximum of 1°C m^{-1}) in the winter of 2010/2011 and

1 decreased over the course of the winter (Figure 4b). In Sa_Lake_4, the maximum temperature
2 gradient was less than $0.2^{\circ}\text{C m}^{-1}$ and, in contrast, increased over the course of the winter
3 (Figure 5c). The waters in both lakes remained stratified during the winter, with gradual
4 overall cooling of the stratified profile continuing until the end of winter.

5 **4.3 Spring**

6 The snow cover on the tundra landscape was usually very thin during the winter (< 0.5 m) and
7 had usually thawed by the end of May or early June. Field observations during a number of
8 spring field campaigns showed that the frozen surfaces of the lakes were normally kept snow-
9 free by wind action. It is interesting to note that the under-ice warming of the water column
10 (Figures 4b, 5c) started as early as the beginning of March (e.g., in 2012), when air
11 temperatures were still well below 0°C , as a result of strong solar radiation input through the
12 ice. A temperature increase of about 4°C over the 6 week period prior to ice break-up is equal
13 to an energy input of about 30 W m^{-2} . With solar radiation returning after the polar night, the
14 shortwave net radiation on the ice surface is about 50 W m^{-2} in March and increases to about
15 300 W m^{-2} by the end of May or the beginning of June (Figure 3b). The net shortwave
16 radiation penetrating to the water column is thus reduced by about 15-20% as a result of
17 transmission through the ice cover. Radiation can penetrate to great water depths depending
18 on the optical properties of the lake water. Assuming light extinction in the water column to
19 be 0.5 m^{-1} , about 13% of the radiation penetrating the ice cover (or $\sim 4 \text{ W m}^{-2}$) will reach the
20 lake floor beneath 4 m of water. The solar radiative heating of the water (still below its
21 maximum density at 4°C) and subsequent convective mixing effectively reduced the
22 temperature gradient beneath the ice cover to less than $0.5^{\circ}\text{C m}^{-1}$ for Sa_Lake_1 and less than
23 $0.1^{\circ}\text{C m}^{-1}$ for Sa_Lake_4 (Figures 4b & 5c), this being a well-known mechanism in ice-
24 covered fresh water lakes during spring (Mironov et al., 2002; Kirillin et al., 2012). Continued
25 solar radiation and air temperature warming induce lake ice melt, which can also be
26 accelerated by high wind speeds. For example, in 2009 the ice cover on Sa_Lake_1 was
27 observed to drift, break-up, shrink, and then disappear, over the course of just a few days due
28 to strong, warm winds. Satellite radar observations from 2011 show that the ice cover break-
29 up occurred over a period of about 10 days from the beginning of June, starting with the
30 formation of a moat. On 10th June all lakes had an ice cover with a moat (i.e. an unfrozen ring
31 close to the shoreline); on 21st June, Sa_Lakes 1, 2, and 3 were ice free but the largest and
32 deepest lakes (Ku_Lake_1 and Sa_Lake_4) still had 40-50% ice cover (Table 1). Complete

1 mixing of the water, as indicated by the first isothermal conditions after the winter
2 stratification (Table 1), had already occurred during the early part of ice break-up (Table 1;
3 Figures 4b, 5c). The lakes were usually ice free by the middle or end of June (Table 1).

4 Seasonal flooding by the Lena River was an additional process that had an important effect on
5 the water temperatures in Sa_Lake_4 (which was formed in a former river channel) and
6 Sa_Lake_1. River ice break-up and flooding took place at the end of May in all three years,
7 when the lakes were still ice covered (Table 1). Lena River temperatures recorded over a
8 complete year (2009-2010) showed that the river temperatures remained around 0°C during
9 the winter, warmed up briefly for about 2 days to a peak temperature of 1.1°C (31 May 2010)
10 and then cooled again to 0°C before steadily increasing thereafter to reach a maximum of
11 19.4°C on 20 July 2010 (Figure 5a). Radiative under-ice warming and convection in
12 Sa_Lake_4 continued until lake ice break-up in 2010, but this spring under-ice warming was
13 interrupted in both 2011 and 2012 by intense flooding with cold Lena River water, as
14 indicated by both the temperature profiles and the water depth data (Figure 5b). The water
15 level in this lake rose by about 1 m over the course of a few hours (28-29 May 2011 & 27-28
16 May 2012), returning to the original level within 4-5 days. Concomitant with water level rise
17 in Sa_Lake_4, the water temperatures fell to 0°C in the upper sensors (immediately beneath
18 the ice). Lake_Sa_1 was also connected to the river during the flood events, as can be
19 recognized by the slight increase in water depth at the end of May in 2010 and 2011 (no water
20 depth data are available for 2012), but the increase was less than in Sa_Lake_4 (< 10 cm
21 variation; Figure 4a).

22 **4.4 Summer**

23 During the summer months positive air temperatures and continuous heat input from solar
24 radiation steadily raised the water temperatures of the lakes at all depths, until September.
25 Heat input from net shortwave radiation supplied about 150 W m⁻² in mid-July (Figure 3).
26 Maximum air temperatures occurred over very short (daytime) periods, reaching up to more
27 than 25°C. The highest air temperatures were recorded in July 2010, reaching a maximum of
28 31.9°C on 5th July.

29 All of the lakes experienced short periods of thermal stratification during the summer, which
30 varied both between the lakes and between the summers; the highest temperature gradient
31 reached was about 5°C m⁻¹ in the deepest lake, Sa_Lake_4 (Figure 5). Maximum water

1 temperatures of around 20°C were usually reached in mid-July, with up to 22°C recorded for
2 the shallow lake (Sa_Lake_3). Mean monthly bottom temperatures during periods with no ice
3 cover ranged between 4°C and 15°C (Figure 6), and can therefore be considerable higher
4 during the summer than their annual means (Table 1).

5 The monthly bottom temperatures for some lakes were also warmer than the corresponding
6 monthly air temperatures (Figure 6), confirming that radiation input is an important additional
7 energy source, as well as effective mixing of the lake waters. Starting with colder mean
8 bottom temperature in July, gradual warming creates warmest mean bottom temperatures in
9 the deepest lake (Sa_Lake_4) in August and in the shallowest lake (Sa_Lake_3) in July. For
10 all other lakes, maximum bottom temperatures occur either in July or August, depending on
11 the timing of ice break up and the lake's seasonal energy balance.

12 The Wedderburn numbers are in agreement with the observed short periods of weak
13 stratification during the ice-free period (Figures 4c, 5d). Remarkably, Wd remain rather low
14 throughout the whole summer (between 1 and 8 for Sa_Lake_1 and Sa_Lake_4) and there are
15 even short periods with $Wd < 1$. These Wd values indicate that buoyancy and wind stress
16 were almost in equilibrium, suggesting favorable conditions for occasional upwelling of the
17 thermocline along the upwind shorelines of the lakes, which would make an additional
18 contribution to the mixing of water in the lakes and to the heat/mass exchange between the
19 lakes and the atmosphere. During short periods with $Wd < 1$ the wind stress is much greater
20 than the buoyancy, effectively destroying the thermal stratification.

21 **4.5 Lake heat content**

22 The heat content in the investigated lakes at times varied by up to +/- 50 MJ m⁻² over just a
23 few days (Figure 7), with the maximum heat content being reached at the end of July or in
24 early August. The summer heat income of the lakes was of the order of 100 to 400 MJ m⁻² and
25 had a linear relationship with their depths (see Equation 1). The winter heat income of the
26 lake water beneath the ice cover varied between 50 and 150 MJ m⁻², not including the heat
27 transfer associated with the formation of the ice cover. However, if a 2 m thick ice cover is
28 taken into account (which is especially important for Arctic lakes; Wetzel, 2001), the annual
29 heat budget can reach up to about 1 GJ m⁻² (Table 1).

30 Sa_Lake_4, which can be subjected to substantial seasonal flooding during spring, showed a
31 reduction in heat content of about 100 MJ m⁻² (in 2010 and 2011) within a few hours, thus

1 suppressing the ongoing radiative warming of the lake water. Although the Lena River carries
2 a substantial amount of heat into its delta every year ($\sim 0.49 * 10^{12} \text{ J s}^{-1}$; Alekseevsky, 2007)
3 due to very warm summer temperatures, the flooding of the lakes occurs when its
4 temperatures are at their coldest.

5 **4.6 Modeled seasonal lake thermal dynamics**

6 A comparative analysis of the modeling results and observational data has revealed the
7 capabilities of, and flaws in, the use of one-dimensional modeling to reproduce the thermal
8 dynamics of lakes formed on permafrost, as well as providing additional quantitative insights
9 into the major mechanisms governing the seasonal thermal dynamics of Siberian lakes. The
10 FLake model results for the Sa_Lake_1 over a period of 2 years (2009-2011) have been in
11 overall good agreement with on-site observations with regard to seasonal variations in lake
12 temperatures, the mean and maximum temperatures in winter and summer, and the durations
13 of the open water and ice cover seasons (Figure 8a-c).

14 To quantify the model performance for thermokarst lakes we applied standard measures (e.g.
15 Thiery et al. 2014) of the model's ability to reproduce the observed mean temperature (T_m),
16 the standard deviation ratio ($SD_{\text{model}}/SD_{\text{obs}}$), the centered root mean squared error (RMSEc),
17 and the Pearson correlation coefficient (r). In contrast to other lake model evaluations using
18 surface temperature T_s (for example, from African and West European lakes), we used T_m
19 since no temperature probes were installed at the surface due to the seasonal ice cover. FLake
20 demonstrated good performance with regard to the mean lake temperature. The statistics—
21 Pearson correlation coefficient $r = 0.97$, $SD_{\text{model}}/SD_{\text{obs}} 1.28$, RMSE 1.49 °C are slightly worse
22 than those reported previously for temperate lakes ($r = 0.988$; Stepanenko et al., 2010) and
23 better than FLake performance on deep tropical lakes ($r = 0.78$, $SD_{\text{model}}/SD_{\text{obs}} 1.25$, RMSE
24 0.75 °C; Thiery et al., 2014). The model reproduced summer stratification during the ice free
25 period ($r = 0.93$, $SD_{\text{model}}/SD_{\text{obs}} 1.25$, RMSE 1.82 °C). Solar heating of the water below the ice
26 is not included in the model and thus the agreement between model and observations is lower
27 during the ice-covered period ($r = -0.42$, $SD_{\text{model}}/SD_{\text{obs}} 0.37$, RMSE 0.66 °C). The resulting
28 uncertainties in the ice break up prediction affect also the model performance with regard to
29 the lake heat content at the beginning of the open water period in early summer (Figure 8). As
30 thermal dynamics under the ice cover are crudely reproduced by the majority of 1-
31 dimensional lake models used in coupled climate modeling systems (Stepanenko et al., 2010),
32 estimation of the role played by thermokarst lakes in regional climate requires integration of a

1 cost-effective and physically sound sub-model of winter lake thermodynamics into lake
2 parameterization schemes for climate models (e.g. Oveisy and Boegman 2014).

3

4 **4.6.1 Open water period and summer stratification**

5 The duration of the warming and cooling periods, as well as the mean water temperatures
6 during the autumn cooling, are well simulated by the model suggesting that the model
7 adequately captures the net heat storage of the lakes. The model was also able to reproduce
8 the development of weak thermal stratification in summer (i.e. the short periods during which
9 the bottom temperatures differed from the mean temperatures of the lakes in June and July,
10 2010 and 2011: Figure 8c). The largest discrepancies in the water temperatures produced by
11 the model occurred during the period of spring warming, with maximum deviations of about
12 6°C from the measured mean temperatures (Figure 8). These deviations can be explained by
13 the ice break-up being modeled too early, with subsequent early warming of the lake. Lake
14 temperatures were consequently consistently overestimated during the warming period in
15 2010.

16 **4.6.2 Ice duration and thickness, and water temperatures beneath the ice** 17 **cover**

18 The mean rate of ice growth modeled with FLake was about 0.92 cm day⁻¹ for 2010
19 (minimum 0.021 cm day⁻¹, maximum 8 cm day⁻¹) and 0.89 cm day⁻¹ for 2011 (minimum
20 0.026 cm day⁻¹, maximum 4.6 cm day⁻¹), with the maximum thickness of ice cover remaining
21 below 2 m. The modeled ice thickness of no more than 2 m agrees well with the temperature
22 data from the sensor located 4 m above the sediment (approximately 2 m from the lake
23 surface) in Sa_Lake_1 (Figure 4b). This sensor did not record any freezing in 2010 or 2011,
24 but in 2012 the sensor froze into the lake ice (Figure 4b), recording sub-zero temperatures and
25 thus indicating thicker ice (> 2 m) in 2012.

26 The modeled melting of the ice cover in spring and subsequent warming of lake temperatures
27 is, in general, well reproduced by the model. The measured development of under-ice bottom
28 temperatures (with warming following the onset of ice cover formation, followed by a later
29 winter cooling) is only partly reproduced in the modeled results due to rather simplified
30 parameterization of the under-ice thermodynamics in the FLake model, with a linear vertical

1 temperature profile in the ice-covered water column and no solar radiation penetrating the ice
2 cover.

3 **4.6.3 Thermal properties of the lake sediments and water-sediment heat flux**

4 Heat conduction from a lake's water column to the underlying sediment is a key
5 thermodynamic process for understanding the role of lakes in the permafrost landscape. The
6 Flake model incorporates simulation of seasonal temperature variations within the thermally
7 active sediment layer, based on an assumption of thermal equilibrium in the sediment over
8 longer-than-seasonal time scales (i.e. a constant temperature beneath the seasonally thermally
9 active sediment layer, ensuring zero mean annual flux across the water-sediment boundary;
10 Golosov and Kirillin, 2010). Since this thermal equilibrium does not necessarily exist in lakes
11 on permafrost, we performed two separate model experiments with different thermal
12 conditions beneath the lakes, based on temperature profiles measured in lake sediments at
13 comparable sites in the Lena River Delta (Grigoriev 1993; Figure 9). While the sediment
14 temperature beneath the shallow lake fell to below 0°C at about 2 m depth and reached -6°C
15 at 15 m depth, the temperatures beneath the deeper lake indicated an unfrozen layer to about
16 25 m depth, with a maximum temperature of about 4.5°C at a depth of about 3 m beneath the
17 lake floor (Figure 9 a, b). The reported temperatures at depth, where seasonal variations were
18 minimal, ranged from -6°C beneath the 1 m deep lake to 4°C beneath the 5 m deep lake.
19 Using the measured temperature profile below the 5 m deep lake, the thickness of the
20 sediment layer with appreciable seasonal variations in temperature was estimated to be ~6 m
21 (Figure 9 b). The FLake modeled heat flux at the lake-sediment boundary for different ground
22 temperatures revealed two characteristic seasonal patterns of lake-permafrost heat exchange:
23 the flux across the frozen sediment beneath the shallow lake was directed downwards during
24 the summer, with a magnitude of up to 4 W m⁻², the fast release of heat from the sediment
25 during autumn cooling, and the water-sediment heat flux of ~0 W m⁻² during the entire ice-
26 covered period (Figure 9 c). This seasonal pattern suggests an annually positive heat budget
27 of the under-lake ground and thawing of the permafrost, which is continuously heated by the
28 lake above. For a lake with deep temperatures approaching 4°C, the annual mean flux across
29 the sediment tended towards zero, with maximum downward fluxes in summer of 3 W m⁻², a
30 maximum of 7 W m⁻² heat released back into the water column during early freeze back, and
31 a continuous low rate of < 1 W m⁻² during the ice-covered winter (Figure 9 d). In the absence
32 of any additional information available on the ground temperatures under Sa_Lake_1, the

1 latter case was adopted for the longer model run (Figures 8b, c), with an “equilibrium state”
2 suggesting little or no permafrost thawing beneath the lake. The maximum modeled heat flux
3 at the sediment-water interface was about 4 W m^{-2} into the sediment (in summer) and about 7
4 W m^{-2} (to almost zero) from the sediment into the water column during the ice-covered
5 period. The rapidly changing (negative) hourly heat fluxes during the fall cooling period were
6 due to rapid cooling of the water column, which could not be reproduced by the model.

7 Overall, the calculated energy density for the lake with mean annual water temperature of 3°C
8 is about 65 MJ m^{-3} , thus more than six times the amount for the permafrost soil of about 10
9 MJ m^{-3} . Lakes are therefore effective for energy storage compared to the frozen landscape,
10 and the fraction of landscape covered by thermokarst lakes has the potential to significantly
11 affect the land-atmosphere energy exchange.

12

13

14 **5 Discussion**

15 Lakes can be considered to represent “hot spots” in the permafrost landscape. This study has
16 demonstrated that the investigated lakes remain unfrozen throughout the winter and have
17 mean bottom water temperatures (between 2.7 to 4.0°C) that are significantly warmer than the
18 mean annual air temperature ($\sim -13^\circ\text{C}$) or the permafrost temperature (-9.2°C at 10.7 m
19 depth). This is in agreement with observations made by Jorgenson et al. (2010) who reported
20 thermokarst lake-bottom temperatures in Alaska that were up to 10°C warmer than the mean
21 annual air temperatures. Harris (2002) attributed the anomalously high mean annual
22 temperature in a shallow lake in western Canada to convective heat exchange and the
23 absorption of radiation through the water column. Mean annual lake-bottom temperatures in
24 northern Alaska also showed a similar range of values (Arp et al. 2012; CALON), and this
25 range has therefore been used in previous modeling studies to estimate the development of
26 talik (Burn, 2002; Ling and Zhang, 2003). Differences in heat content are related to
27 morphometric parameters, particularly to water depth. Burn (2002) found mean annual lake-
28 bottom temperatures of between 1.5°C and 4.8°C for the deeper pools in tundra lakes on
29 Richards Island (north-western Canada). Ensom et al. (2012) reported mean annual bottom
30 temperatures of between 3.4°C and 5.5°C from a number of lakes and channels in the
31 Mackenzie Delta (Canada) and computed that 60% of the lakes maintained taliks.

1 Mean bottom lake temperatures, which ranged between 2.7 and 4 °C in this study, depend on
2 lake depth and are important for constraining future numerical modeling experiments on talik
3 development. Our study also confirms previous findings that there is a “critical lake depth”
4 (lake depth > winter ice cover thickness) for water to remain unfrozen beneath the ice cover
5 (Arp et al., 2012; Burn, 2002). All lakes in this study had a depth > 3 m, which exceeds the
6 maximum ice thickness of about 2 m.

7 The bottom temperatures in the lakes varied significantly between summer and winter but
8 their annual mean temperatures and temperature dynamics were similar despite the range of
9 morphometric and geomorphological characteristics. The Wd numbers indicated that the lakes
10 were all well-mixed during the summer periods, and it can therefore be assumed that both
11 heat and dissolved gases, in particular, oxygen, are effectively transported through the water
12 column. This assumption is supported by the measured oxygen concentrations in these lakes,
13 which ranged between 8 and 10 mg l⁻¹, and the lack of any detected vertical stratification (R.
14 Osudar, personal communication, 2015).

15 We observed and simulated short stratification periods in summer in the studied lakes
16 (Figures 4 & 5). The effect of these stratification events on lake biogeochemistry is probably
17 the major physical factor affecting biogeochemical processes in lakes. In particular, the
18 duration of the thermal stratification in summer affects the concentration and vertical
19 distribution of dissolved oxygen. Longer summer stratification provokes deep anoxia and
20 favors methanogenesis in the deep water column and upper sediment (Golosov et al., 2012).
21 Under equal climatic forcing, lake depth is the primary factor determining the duration of
22 summer stratification (the second one being the water transparency, Kirillin, 2010).
23 Sensitivity model runs with the lake depth varying in the range 2-12 m using the same
24 meteorological input data from Samoylov demonstrated that lakes in this climatic zone with
25 mean depths >5 m should have dimictic stratification regimes, i.e. develop continuous
26 stratification in summer with duration of 1 month or longer (Figure 10). This also supports the
27 observation of summer stratification in deeper (> 6 m) Alaskan thermokarst lakes (Sepulveda-
28 Jáuregui et al., 2015). In lakes of about 8 m depth or more, the summer stratification duration
29 significantly increases since high thermal inertia prevents vertical mixing during the autumn
30 cooling in August-September (Figure 11).

31 The summer heat budgets of Arctic lakes are much smaller than those of low-latitude lakes.
32 The only previously reported summer heat budget for an Arctic lake (Chandler Lake, Alaska)

1 was 240 MJ m^{-2} , which lies in the same range as the heat budgets in this study (Wetzel, 2001).
2 In contrast, the summer heat budget for a large lake such as Lake Superior on the Canada-
3 USA border is much larger at about 1.3 GJ m^{-2} . In comparison, the annual heat budget of
4 Lake Baikal in Siberia is estimated to be about 2.7 GJ m^{-2} (Wetzel, 2001). The total annual
5 heat budget for all of the investigated lakes (including the latent heat of the ice cover)
6 amounts up to about 1 GJ m^{-2} (Table 1). In view of the large proportion of land covered by
7 water bodies in this landscape (25%) and the volumes of water that they contain, their energy
8 storage and turnover within the permafrost landscape are of considerable significance.
9 Furthermore, changes in the heat content of lakes occur much more rapidly than changes in
10 the heat content of the surrounding permafrost soils as a result of efficient energy absorption
11 and effective mixing. In contrast, progressive deepening of the seasonally thawing upper layer
12 of permafrost (the active layer) of the polygonal tundra landscape at this site takes several
13 months and only reaches a maximum thaw depth of about 0.6 m (Boike et al., 2013). Lakes
14 also have an important effect on the subsurface thermal conditions beneath the lake and
15 potentially also in the surrounding permafrost. Our results show that, during the summer, heat
16 is continuously transferred from lake water into the bottom sediment. The importance of
17 summer heat gain and its dissipation into the water body and the underlying sediment was
18 first discussed by Vtyurina (1960), using data from a 12 m deep lake in Siberia. Her findings
19 showed heat fluxes directed into the sediments during winter (Figure 5 in Vtyurina, 1960; also
20 reported in Grosse et al., 2013) which, according to our findings, is an indicator of permafrost
21 thaw. Our modeling results, however, suggest that the temperature increase associated with
22 permafrost thaw eventually results in a net annual heat equilibrium between deeper lakes and
23 the underlying sediments, characterized by a continuous negative heat flux (i.e. heat loss from
24 the sediment into the water column) during the long ice-covered winter and heat gain by the
25 sediment during the open water summer period. The warming of lake-bottom temperatures
26 with the onset of ice cover was initially attributed by Brewer (1958) to heating by the
27 shortwave solar radiation and by Mortimer and Mackereth (1958) to the heat release from the
28 lake sediment. Our observed near-bottom temperatures increased beneath the ice cover and
29 the modeling experiments suggested this warming was solely due to heat flow from the
30 sediment, with typical rates of $< 10 \text{ W m}^{-2}$. However, the heat flux from the sediment in
31 tundra lakes appears to decay within less than one month, which is much faster than in ice-
32 covered lakes of the temperate and boreal climates (cf. Rizk et al. 2014), and is followed by a

1 gradual decrease of the deep water temperatures. The latter is not reproduced by the
2 parameterized sediment module of FLake.

3

4 Our numerical modeling of the thermal dynamics of lakes has shown that the basic processes
5 can be accurately reproduced for the summer. However, the model parameters that yielded the
6 best fit for the seasonal heat budget and ice cover duration resulted in less accurate predictions
7 of the bottom temperature under ice. Lake temperatures increase, starting in spring 1-2
8 months before ice-off, apparently by radiative solar heating. This temperature increase
9 suggests that radiation can make a significant direct contribution to sediment heating in
10 shallow and clear-water thermokarst lakes – a contribution that is usually neglected in lake
11 models. The concept of self-similarity cannot account for the permafrost-talik specific lake
12 processes, such as (i) warming of bottom waters immediately following onset of ice formation
13 and (ii) phase change in the lake's frozen sediment, i.e. annual freeze thaw processes and
14 thawing at the talik-permafrost boundary. While the short period of warming of bottom water
15 is due to heat flux from the sediment into the water body, the cooling in winter from mid-
16 winter onwards suggests a loss of heat. This heat loss may occur through transmission into
17 both the sediment and the atmosphere, the latter being of minor importance due to isolation of
18 the water column by the ice cover. Further investigations into these processes of warming and
19 subsequent gradual cooling under the ice cover would require a more advanced lake model
20 that is able to take into account deep, continuously frozen sediments and characteristic
21 processes such as thawing.

22

23 **6 Summary and conclusions**

24 We have measured and modeled the thermal dynamics of lakes in the Lena River Delta of
25 northern Siberia over a three year period (2009-2012), with the objective of understanding
26 and quantifying the important thermal processes that operate in this permafrost environment.
27 The investigated lakes were situated in two different geomorphologic settings (sediments of
28 the Pleistocene Ice Complex and on a younger river terrace) with a range of morphometric
29 characteristics. Some of the lakes were seasonally connected to the Lena River through high
30 floods that occurred during spring. Such annual flooding of these lakes by cold river water
31 results in a significant reduction in the ongoing warming (and thus sensible heat storage),

1 depending on the magnitude of the flooding. A schematic summary of our results is provided
2 in Figure 12.

3 The lakes were shown to receive substantial energy for warming from net shortwave radiation
4 during the summer. Warming also occurs during the ice cover period in spring, resulting in
5 convective mixing beneath the ice cover. Mixing also occurs following ice break-up, during
6 the summer, and during the fall cooling, resulting in efficient heat transfer to bottom waters
7 and across the sediment-water interface. Numerical modeling suggests that the annual mean
8 net heat flux across the bottom sediment boundary is approximately zero, with positive
9 summer downward fluxes during the ice-free period (4 months) and heat-release back into the
10 water column at much lower rates during the ice-covered period (8 months). Overall, the ice
11 formation and thaw together account for most of the annual variations in a lake's heat content.
12 Furthermore, their timing and durations determine the magnitude and direction of bottom
13 sediment heat fluxes and the timing of water column mixing. Future warming may result in
14 changes to the ice cover but may also produce more pronounced summer stratification, thus
15 potentially reducing the heat input into the sediment layers.

16 In view of the large area covered by water bodies in permafrost landscapes (25% of the land
17 surface) and their efficiency at energy absorption and mixing, these water bodies are clearly
18 of considerable importance with respect to energy storage and turnover, atmospheric fluxes,
19 and sediment heat fluxes in permafrost landscapes.

20 The investigated thermokarst lakes are representative of Arctic tundra lowlands characterized
21 by thermokarst processes that are common for large regions in Central and East Siberia,
22 Interior and Northern Alaska as well as Northwest Canada. Despite their importance,
23 however, lakes are not yet included in earth system models. Future work should therefore
24 include lakes in these models and test their sensitivity to possible future changes in climate.

25

26 Author contributions: J. Boike designed the research and led the discussions, supported by G.
27 Kirilin and M.Langer. The FLake modeling was carried out by G. Kirilin and C. Georgi. The
28 paper was written by J.Boike, with comments from all authors.

29

30 Acknowledgements: The logistical support provided by the Russian Research station on
31 Samoylov Island is gratefully acknowledged. Field support, including data collection, was

1 provided by Grigoriy Soloviev, Waldemar Schneider, Günther Stoof, and Karoline
2 Wischnewski. Elizabeth Miller, Max Heikenfeld, Wil Lieberman-Cribbin and Stephan Lange
3 assisted with the data analysis and helpful discussions. The authors acknowledge the financial
4 support provided through the European Union's FP7-ENV PAGE21 project under contract
5 number GA282700, and through the Feodor Lynen grant from the Alexander-von-Humboldt
6 Foundation awarded to Moritz Langer. The research was carried out under the Russian
7 government's Program of Competitive Growth, Kazan Federal University.

1 **References**

- 2 Alekseevsky, N. I. (Ed.): Geocological state of Russian Arctic coast and their safety of
3 nature management (in Russian), GEOS Publ., Moscow, Russia, 586 pp., 2007.
- 4 Abnizova, A., Siemens, J., Langer, M., and Boike, J.: Small ponds with major impact: The
5 relevance of ponds and lakes in permafrost landscapes to carbon dioxide emissions, *Global*
6 *Biogeochem. Cycles*, 26, GB2041, doi: 10.1029/2011gb004237, 2012.
- 7 Alerstam, T., Gudmundsson, G. A., Green, M., and Hedenström, A.: Migration along
8 orthodromic sun compass routes by arctic birds, *Science*, 291, 300-303, 2001.
- 9 Are F. E.: Thermal regime of small thermokarst lakes in the Siberian Taiga zone (for example
10 of Central Yakutia) (in Russian), Collection of papers "Lakes of Cryolithozone of Siberia",
11 edited by: Are F.E., Nauka, Siberian brunch, 98-116, 1974.
- 12 Arp, C. D., Jones, B. M., Whitman, M., Larsen, A., and Urban, F. E.: Lake Temperature and
13 Ice Cover Regimes in the Alaskan Subarctic and Arctic: Integrated Monitoring, Remote
14 Sensing, and Modeling, *J. Am. Water Resour. Assoc.*, 46, 777-791, doi: 15, 10.1111/j.1752-
15 1688.2010.00451.x, 2010.
- 16 Arp, C. D., Jones, B. M., Lu, Z., and Whitman, M. S.: Shifting balance of thermokarst lake
17 ice regimes across the Arctic Coastal Plain of northern Alaska, *Geophys. Res. Lett.*, 39, doi:
18 10.1029/2012gl052518, 2012.
- 19 Boike, J., Wille, C., and Abnizova, A.: Climatology and summer energy and water balance of
20 polygonal tundra in the Lena River Delta, Siberia, *J. Geophys. Res.*, 113, G03025,
21 doi:10.1029/2007JG000540, 2008.
- 22 Boike, J., Kattenstroth, B., Abramova, K., Bornemann, N., Chetverova, A., Fedorova, I.,
23 Fröb, K., Grigoriev, M., Grüber, M., Kutzbach, L., Langer, M., Minke, M., Muster, S., Piel,
24 K., Pfeiffer, E. M., Stoof, G., Westermann, S., Wischnewski, K., Wille, C., and Hubberten, H.
25 W.: Baseline characteristics of climate, permafrost and land cover from a new permafrost
26 observatory in the Lena River Delta, Siberia (1998-2011), *Biogeosciences*, 10, 2105-2128,
27 doi: 10.5194/bg-10-2105-2013, 2013.
- 28 Burn, C. R.: Tundra Lakes and Permafrost, Richards Island, Western Arctic Coast, Canada,
29 *Canadian Journal Earth Science*, 39, 1281-1298, doi:10.1139/E02-035, 2002.

1 Burn, C. R.: Lake-bottom Thermal Regimes, Western Arctic Coast, Canada, Permafr.
2 Periglac. Proc., 16, 355–367, doi: 10.1002/PPP.542, 2005.

3 Brewer, M. C.: The thermal regime of an arctic lake, EOS Transactions ,American
4 Geophysical Union, 39, 2, 278-284, doi: 10.1029/TR039i002p00278, 1958: Costard, F., and
5 Gautier, E.: The Lena River: Hydromorphodynamic Features in a Deep Permafrost Zone, in:
6 Large Rivers: Geomorphology and Management, edited by: Gupta, A., John Wiley & Sons,
7 Ltd, West Sussex, England, 225-233, 2007.

8 Chetverova, A., Fedorova, I., Potapova, T., Boike, J.: Hydrological and geochemical features
9 of lakes of Samoylov Island of the Lena River Delta./ Proceedings of AARI, № 1 (95), 97-
10 110, 2013 (in Russian).

11 Ensom, T. P., Burn, C. R., and Kokelj, S. V.: Lake- and channel-bottom temperatures in the
12 Mackenzie Delta, Northwest Territories, Can. J. Earth Sci., 49, 16, 963-978, doi:
13 10.1139/e2012-001, 2012.

14 Fedorova, I., Chetverova, A., Bolshiyarov, D., Makarov, A., Boike, J., Heim, B.,
15 Morgenstern, A., Overduin, P. P., Wegner, C., Kashina, V., Eulenburg, A., Dobrotina, E., and
16 Sidorina, I.: Lena Delta hydrology and geochemistry: long-term hydrological data and recent
17 field observations, Biogeosciences, 12, 345-363, doi: 10.5194/bg-12-345-2015, 2015.

18 Golosov, S., and Kirillin, G.: A parameterized model of heat storage by lake sediments,
19 Environ. Model. Software, 25, 793-801, doi: 10.1016/j.envsoft.2010.01.002, 2010.

20 Golosov, S., Terzhevik, A., Zverev, I., Kirillin, G. and Engelhardt, C.: Climate change impact
21 on thermal and oxygen regime of shallow lakes. Tellus A, 64, 17264, doi:
22 10.3402/tellusa.v64i0.17264, 2012.

23 Gordeev, V. V., and Sidorov, I. S.: Concentrations of major elements and their outflow into
24 the Laptev Sea by the Lena River, Marine Chemistry, 43, 33-45, 1993.

25 Grigoriev, M.: Cryomorphogenesis of the Lena River mouth area (in Russian), Siberian
26 Branch, USSR Academy of Sciences, Yakutsk, 176 pp., 1993.

27 Grigoriev, N. F.: The temperature of permafrost in the Lena delta basin–deposit conditions
28 and properties of the permafrost in Yakutia (in Russian), Yakutsk, 2, 97-101, 1960.

29 Grigoriev, N. F. Perennially frozen rocks of the maritime lowlands of Yakutia (in Russian),
30 Moscow, Nauka, 80, pp, 1966.

1 Grosse, G., Jones, B., and Arp, C. D.: Thermokarst Lakes, Drainage, and Drained Basins, in:
2 Treatise on Geomorphology, edited by Giardino, R. & Harbor, J., 8 Glacial and Periglacial
3 Geomorphology, 29, 325-353, Academic Press, San Diego, CA, doi: 10.1016/B978-0-12-
4 374739-6.00216-5, 2013.

5 Harris, S. A.: Causes and consequences of rapid thermokarst development in permafrost or
6 glacial terrain, *Permafr. Periglac. Proc.*, 13, 237-242, doi: 10.1002/ppp.419, 2002.

7 Hinkel, K. M., Lenters, J. D., Sheng, Y., Lyons, E. A., Beck, R. A., Eisner, W. R., Maurer, E.
8 F., Wang, J., and Potter, B. L.: Thermokarst Lakes on the Arctic Coastal Plain of Alaska:
9 Spatial and Temporal Variability in Summer Water Temperature, *Permafr. Periglac. Proc.*, 23,
10 207-217, doi: 10.1002/ppp.1743, 2012.

11 Hobbie, J. E., and Kling, G. W.: Alaska's changing Arctic: Ecological consequences for
12 tundra, streams, and lakes, Oxford University Press, 352 pp., 2014.

13 Jeffries, M. O., Zhang, T., Frey, K., and Kozlenko, N.: Estimating Late-Winter Heat Flow to
14 the Atmosphere from the Lake-Dominated Alaskan North Slope, *Journal Glaciology*, 45, 315-
15 347, 1999.

16 Jorgenson, M. T., Romanovsky, V., Harden, J., Shur, Y., O'Donnell, J., Schuur, E. A. G.,
17 Kanevskiy, M., and Marchenko, S.: Resilience and vulnerability of permafrost to climate
18 change, *Canadian Journal of Forest Research*, 40, 1219-1236, doi: 10.1139/x10-060, 2010.

19 Kalnay, E., Kanamitsu, M., Kistler, R., Collins, W., Deaven, D., Gandin, L., Iredell, M., Saha,
20 S., White, G., Woollen, J., Zhu, Y., Leetmaa, A., Reynolds, R., Chelliah, M., Ebisuzaki, W.,
21 Higgins, W., Janowiak, J., Mo, K. C., Ropelewski, C., Wang, J., Jenne, R., and Joseph, D.:
22 The NCEP/NCAR 40-Year Reanalysis Project, *Bull. Am. Meteorol. Soc.*, 77, 437-471, 1996.

23 Keatley, B. E., Douglas, M. S. V., and Smol, J. P.: Physical and chemical limnological
24 characteristics of lakes and ponds across environmental gradients on Melville Island,
25 Nunavut/N.W.T., High Arctic Canada, *Fundamental and Applied Limnology - Archiv für*
26 *Hydrobiologie*, 168, 355–376, doi: 10.1127/1863-9135/2007/0168-0355, 2007.

27 Kirillin, G.: Modeling the impact of global warming on water temperature and seasonal
28 mixing regimes in small temperate lakes. *Boreal Environ. Res*, 15, 279-293, 2010.

29

1 Kirillin, G., Leppäranta, M., Terzhevik, A., Granin, N., Bernhardt, J., Engelhardt, C.,
2 Efremova, T., Golosov, S., Palshin, N., and Sherstyankin, P.: Physics of seasonally ice-
3 covered lakes: a review, *Aquat. Sci.*, 74, 659-682, 2012.

4 Lachenbruch, A. H.: Mechanics of thermal contraction cracks and ice-wedge polygons in
5 permafrost, *Special papers*, 70, Geological Society of America, New York, 69 pp., 1962.

6 Langer, M., Westermann, S., Muster, S., Piel, K., and Boike, J.: The surface energy balance
7 of a polygonal tundra site in northern Siberia Part 1: Spring to fall, *The Cryosphere*, 5, 151-
8 171, doi: 10.5194/tc-5-151-2011, 2011a.

9 Langer, M., Westermann, S., Muster, S., Piel, K., and Boike, J.: The surface energy balance
10 of a polygonal tundra site in northern Siberia - Part 2: Winter, *The Cryosphere*, 5, 509-524,
11 doi: 10.5194/tc-5-509-2011, 2011b.

12 Langer, M., Westermann, S., Heikenfeld, M., Dorn, W., and Boike, J.: Satellite-based
13 modeling of permafrost temperatures in a tundra lowland landscape, *Remote Sensing of*
14 *Environment*, 135, 12-24, doi: 10.1016/j.rse.2013.03.011, 2013.

15 Langer, M., Westermann, S., Walter Anthony, K., Wischnewski, K., and Boike, J.: Frozen
16 ponds: production and storage of methane during the Arctic winter in a lowland tundra
17 landscape in northern Siberia, Lena River delta, *Biogeosciences*, 12, 977-990, doi:
18 10.5194/bg-12-977-2015, 2015.

19 Laurion, I., Vincent, W.F., Retamal, L., Dupont, C., Francus, P., MacIntyre, S. & Pienitz, R.:
20 Variability in greenhouse gas emissions from permafrost thaw ponds. *Limnology and*
21 *Oceanography* 55, 115-133, 2010.

22 Lehner, B., and Döll, P.: Development and validation of a global database of lakes, reservoirs
23 and wetlands, *Journal of Hydrology*, 296, 1-22, 2004.

24 Ling, F., and Zhang, T.: Numerical simulation of permafrost thermal regime and talik
25 development under shallow thaw lakes on the Alaskan Arctic Coastal Plain, *J. Geophys. Res.*,
26 108, 4511, doi: 10.1029/2002JD003014, 2003.

27 Luecke, C., Giblin, A. E., Bettez, N. D., Burkart, G. A., Crump, B. C., Evans, M. A., Gettel,
28 G., McIntyre, S., O'Brien, W. J., Rublee, P. A., and King, G. W.: The response of lakes near
29 the Arctic LTER to environmental change, in: *Alaska's changing Arctic: ecological*

1 consequences for tundra, streams, and lakes, edited by: Hobbie, J., and Kling, G. W., Oxford
2 University Press, New York, 238-286, 2014.

3 Martynov, A., Sushama, L. and Laprise, R.: Simulation of temperate freezing lakes by one-
4 dimensional lake models: performance assessment for interactive coupling with regional
5 climate models. *Boreal Environ. Res.*, 15(2), 143-164, 2010.

6 Martynov, A., Sushama, L., Laprise, R., Winger, K., and Dugas, B.: Interactive lakes in the
7 Canadian Regional Climate Model, version 5: the role of lakes in the regional climate of
8 North America, *Tellus A*, 64, 16226, doi: 10.3402/tellusa.v64i0.16226, 2012.

9 Mironov, D. V., Terzhevik, A., Kirillin, G., Jonas, T., Malm, J., and Farmer, D.: Radiatively
10 driven convection in ice-covered lakes: Observations, scaling, and a mixed layer model,
11 *Journal of Geophysical Research: Oceans*, 107, 7, 1-16, doi: 10.1029/2001JC000892, 2002.

12 Mironov, D. V.: Parameterization of lakes in numerical weather prediction. Description of a
13 lake model, COSMO technical report, 2005.

14 Mironov, D., B. Ritter, J.-P. Schulz, M. Buchhold, M. Lange, and E. Machulskaya:
15 Parameterization of sea and lake ice in numerical weather prediction models of the German
16 Weather Service. *Tellus A*, 64, 17330. doi: 10.3402/tellusa.v64i0.17330, 2012

17 Morgenstern, A., Grosse, G., Günther, F., Fedorova, I., and Schirrmeister, L.: Spatial analyses of
18 thermokarst lakes and basins in Yedoma landscapes of the Lena Delta, *The Cryosphere*, 5,
19 849-867, 10.5194/tc-5-849-2011, 2011.

20 Morgenstern, A., Grosse, G., Günther, F., Fedorova, I., and Schirrmeister, L.: Spatial analyses
21 of thermokarst lakes and basins in Yedoma landscapes of the Lena Delta, *The Cryosphere*, 5,
22 849-867, doi:10.5194/tc-5-849-2011, 2011.

23 Morgenstern, A., Ulrich, M., Günther, F., Roessler, S., Fedorova, I. V., Rudaya, N. A.,
24 Wetterich, S., Boike, J., and Schirrmeister, L.: Evolution of thermokarst in East Siberian ice-
25 rich permafrost: A case study, *Geomorphology*, 201, 363-379, doi:
26 10.1016/j.geomorph.2013.07.011, 2013.

27 Mortimer, C. and Mackereth F: Convection and its consequences in ice-covered lakes. *Verh*
28 *Int Ver Limnol*, 13, 923–932, 1958.

29

- 1 Muster, S., Langer, M., Heim, B., Westermann, S., and Boike, J.: Subpixel heterogeneity of
2 ice-wedge polygonal tundra: a multi-scale analysis of land cover and evapotranspiration in the
3 Lena River Delta, Siberia, *Tellus B*, 64, 17301, doi: 10.3402/tellusb.v64i0.17301, 2012.
- 4 Nolan, M., and Brigham-Grette, J.: Basic hydrology, limnology, and meteorology of modern
5 Lake El'gygytgyn, Siberia, *J. Paleolimnol.*, 37, 17-35, doi: 10.1007/s10933-006-9020-y,
6 2006.
- 7 Oveisy, A. and Boegman, L.: One-dimensional simulation of lake and ice dynamics during
8 winter. *J. Limnol.*, 73, doi: 10.4081/jlimnol.2014.903, 2014.
- 9 Pavlov A.V., Tishin M.I.: Heat balance of a large lake and surrounding area in central Yakutia
10 (in Russian), Collection of papers "Structure and thermal regime of frozen rocks", edited by:
11 Katasonova E.G., Pavlov A.V., Nauka, Siberian branch, 53-62 1981.
- 12 Pienitz, R., Smol, J. P., and Lean, D. R. S.: Physical and Chemical limnology of 59 lakes
13 located between the southern Yukon and the Tuktoyaktuk Peninsula, Northwest Territories
14 (Canada), *Can. J. Fish. Aquat. Sci.*, 54, 330-346, 1997.
- 15 Rawlins, M. A., Serreze, M. C., Schroeder, R., Zhang, X., and McDonald, K. C.: Diagnosis of
16 the record discharge of Arctic-draining Eurasian rivers in 2007, *Environmental Research*
17 *Letters*, 4, 1-8, 2009.
- 18 Read, J. S., Hamilton, D. P., Jones, I. D., Muraoka, K., Winslow, L. A., Kroiss, R., Wu, C. H.,
19 and Gaiser, E.: Derivation of lake mixing and stratification indices from high-resolution lake
20 buoy data, *Environ. Model. Software*, 26, 1325-1336, doi: 10.1016/j.envsoft.2011.05.006,
21 2011.
- 22 Rizk, W., Kirillin, G. and Leppäranta, M.: Basin-scale circulation and heat fluxes in ice-
23 covered lakes. *Limnol. Oceanogr.*, 59, 445-464, 2014.
- 24 Sepulveda-Jauregui, A., Walter Anthony, K. M., Martinez-Cruz, K., Greene, S., and
25 Thalasso, F.: Methane and carbon dioxide emissions from 40 lakes along a north-south
26 latitudinal transect in Alaska, *Biogeosciences*, 12, 3197-3223, doi:10.5194/bg-12-3197-2015,
27 2015.
- 28 Schertzer, W. M.: Freshwater Lakes, in: *Surface climates of Canada*, edited by: Bailey, W. G.,
29 Oke, T. R., and Rouse, W. R., McGill-Queens University Press, Montreal, 124-148, 1997.

- 1 Schneider von Deimling, T., Grosse, G., Strauss, J., Schirrmeister, L., Morgenstern, A.,
2 Schaphoff, S., Meinshausen, M., and Boike, J.: Observation-based modelling of permafrost
3 carbon fluxes with accounting for deep carbon deposits and thermokarst activity, *Biogeosci.*
4 *Disc.*, 11, 16599-16643, doi: 10.5194/bgd-11-16599-2014, 2014.
- 5 Schwamborn, G., Rachold, V., and Grigoriev, M. N.: Late Quaternary sedimentation history
6 of the Lena Delta, *Quat. Int.*, 89, 119-134, doi: 10.1016/S1040-6182(01)00084-2, 2002.
- 7 Sobiech, J., Boike, J., and Dierking, W.: Observation of melt onset in an Arctic Tundra
8 landscape using high resolution TerraSAR-X and RADARSAT-2 data, IGARSS, Munich,
9 Germany, 3552–3555, 2012.
- 10 Spiegel, R. H., and Imberger, J. The classification of mixed-layer dynamics of lakes of small
11 to medium size. *Journal of physical oceanography*, 10(7), 1104-1121, 1980.
- 12 Stefan, J.: Über die Theorie der Eisbildung, insbesondere über die Eisbildung im Polarmeere,
13 *Annalen der Physik*, 278, 269-286, 1891.
- 14 Stepanenko, V.M., Goyette, S., Martynov, A., Perroud, M., Fang, X. and Mironov, D.: First
15 steps of a lake model intercomparison Project: LakeMIP. *Bor. Environ. Res.*, 15, 191-202,
16 2010.
- 17 Thiery, W., Stepanenko, V. M., Fang, X., Jöhnk, K. D., Li, Z., Martynov, A., Perroud, M.,
18 Subin, Z. M., Darchambeau, F., Mironov, D., and van Lipzig, N. P. M.: LakeMIP Kivu:
19 evaluating the representation of a large, deep tropical lake by a set of one-dimensional lake
20 models, 2014, doi: 10.3402/tellusa.v66.21390, 2014.
- 21 Vincent, A. C., Mueller, D. R., and Vincent, W. F.: Simulated heat storage in a perennially
22 ice-covered high Arctic lake: Sensitivity to climate change, *J. Geophys. Res.*, 113, C04036,
23 doi: 10.1029/2007JC004360, 2008.
- 24 Vincent, W.F., Pienitz, R., Laurion, I. and Walter Anthony, K.: Climate impacts on Arctic
25 lakes. In: Goldman, C.R., Kumagai, M. and Robarts, R.D. (eds). *Climatic Change and Global*
26 *Warming of Inland Waters: Impacts and Mitigation for Ecosystems and Societies*, John Wiley
27 & Sons, Ltd, Chichester, U.K., 27-42, 2013.
- 28 Vtyurina, E. A.: Temperature regime of the Lake Glubokoe Trudy institute merzlotovedeniya
29 im. V.A. Obrucheva. AN SSSR, Moscow, 132-140, 1960 (in Russian).

- 1 Walsh, S. E., Vavrus, S. J., Foley, J. A., Fisher, V. A., Wynne, R. H., and Lenters, J. D.:
2 Global Patterns of Lake Ice Phenology and Climate: Model Simulation and Observation, *J.*
3 *Geophys. Res.*, 103, 28, 825-828, 1998.
- 4 Walter, K. M., Zimov, S. A., Chanton, J. P., Verbyla, D., and Chapin III, F. S.: Methane
5 bubbling from Siberian thaw lakes as a positive feedback to climate warming, *Nature*, 443,
6 71-75, doi: 10.1038/nature05040, 2006.
- 7 Welch, H. E., and Bergmann, M. A.: Water circulation in small arctic lakes in winter, *Can. J.*
8 *Fish. Aquat. Sci.*, 42, 506-520, 1985.
- 9 Wetterich, S., Schirrmeister, L., Meyer, H., Andreas, F. A., and Mackensen, A.: Arctic
10 freshwater ostracods from modern periglacial environments in the Lena River Delta (Siberian
11 Arctic, Russia): geochemical applications for palaeoenvironmental reconstructions, *J.*
12 *Paleolimnol.*, 39, 427–449, doi: 10.1007/s10933-007-9122-1, 2008.
- 13 Wetzel, R. G.: *Limnology: lake and river ecosystems*, 3rd ed., Gulf Professional Publishing,
14 Orlando, 1006 pp., 2001.
- 15 Yi, S., Wischnewski, K., Langer, M., Muster, S., and Boike, J.: Freeze/thaw processes in
16 complex permafrost landscapes of northern Siberia simulated using the TEM ecosystem
17 model: impact of thermokarst ponds and lakes, *Geoscientific Model Development*, 7, 1671-
18 1689, doi: 10.5194/gmd-7-1671-2014, 2014.
- 19

1 Table 1. Physical and chemical characteristics of the studied lakes in the Lena River Delta,
 2 Siberia

	Sa_Lake_1	Sa_Lake_2	Sa_Lake_3	Sa_Lake_4	Ku_Lake_1
Area [m ²]	39,541	39,991	23,066	47,620	1,730,000 ^a
Max. depth [m]	6.4	5.7	3.4	11.6	3.6 ^a
Mean depth [m]	3	3.1	1.2	4.5	2.4
Volume [m ³]	106,500	103,600	18,800	175,121	3,321,000
Volume/Area [m]	2.7	2.6	0.8	3.7	1.8
Perimeter [m]	1,931	1,471	1,760	1,474	5,170 ^a
Period of data collection	04 July 2009 - 07 Aug. 2012	10 July 2009 - 07 Aug. 2012	13 July 2009 - 14 Aug. 2012	06 July 2009 - 06 Aug. 2012	24 July 2009 - 29 July 2010
Location	126.486 E, 72.373 N	126.496 E, 72.378 N	126.511 E, 72.374 N	126.505 E, 72.369 N	126.177 E, 72.328 N
Start of ice cover formation (temp. diff. from bottom to top > 0.1°C)	05 Oct. 2009 01 Oct. 2010 02 Oct. 2011	1 Oct. 2009 28 Sep. 2010 05 Oct. 2011	04 Oct. 2009 30 Sep. 2010 26 Sep. 2011	04 Oct. 2009 28 Sep. 2010 4 Oct. 2011	04 Oct. 2009 02 Oct. 2010
Start of ice cover break-up (temp. diff. from	04 July 2009 14 June 2010 08 June 2011	12 July 2009 23 June 2010 16 June 2011	24 June 2009 14 June 2010 10 June 2011	07 July 2009 20 June 2010 20 June 2011	24 July 2009 20 June 2010

	15 June 2012	15 June 2012	10 June 2012	21 June 2012	21 June 2012
bottom to top > 0.1°C)					
% ice cover	5 June:100%	5 June: 100%	5 June: 100%	5 June: 95%	5 June: 95%
(satellite radar data ^{b)})	10 June: 95%	10 June: 100%	10 June: 90%	10 June: 95%	10 June: 95%
2011	16 June: 85%	16 June: 90%	16 June: ice free	16 June: 85%	16 June: 90%
	21 June: ice free	21 June: ice free		21 June: 50%	21 June: 40%
					27 June: ice free
2012	27 June: ice free	27 June: ice free	27 June: ice free	27 June: ice free	05 June: 90%
					27 June: ice free
Mean annual bottom temperature [°C] (2010-2011)	3.7	3.6	2.7	2.9	4.0
Winter lake water heat budget [MJ m ⁻²]	93	66	44	145	61
Summer lake water heat budget [MJ m ⁻²]	140	206	161	340	112
Annual lake heat budget [MJ m ⁻²] (2010-2011)	[233] 838	[272] 877	[205] 810	[485] 1090	[173] 778

c, d

Residence time [years] ^e	14	14	4	24	9
Electrical conductivity [$\mu\text{S cm}^{-1}$]	140 ^f	127 ^f	64 ⁱ	185 ^f 59 ^g 80 ^h	30 ⁱ
pH-value ^f	6.99 ^f	6.82 ^f	7.3 ⁱ	6.95 ^f 7.36 ^g 7.28 ^h	7.64 ⁱ

1

2 ^a data provided in Morgenstern et al. (2011, 2013) and <http://doi.pangaea.de/10.1594/PANGAEA.848485>

3 ^b Sobiech et al. (2012) & TerraSar-X data (copyright: DLR, 2011) where available with sufficiently high
4 resolution

5 ^c numbers in brackets represent the total annual lake water budget (sensible heat), without taking into account the
6 latent heat of ice cover formation

7 ^d includes latent heat for the formation of a 2 m ice cover (605 MJ m^{-2})

8 ^e residence time $F = V/E$; roughly approximated by the ratio of the lakes's volume (V) divided by the sum of
9 evapotranspiration (E) and runoff R ($F = V/(E-R)$; Schertzer 1997). Within the study area, the annual
10 evapotranspiration is about ~190 mm and runoff is to be negligible within the overall water balance (Boike et al.,
11 2013)

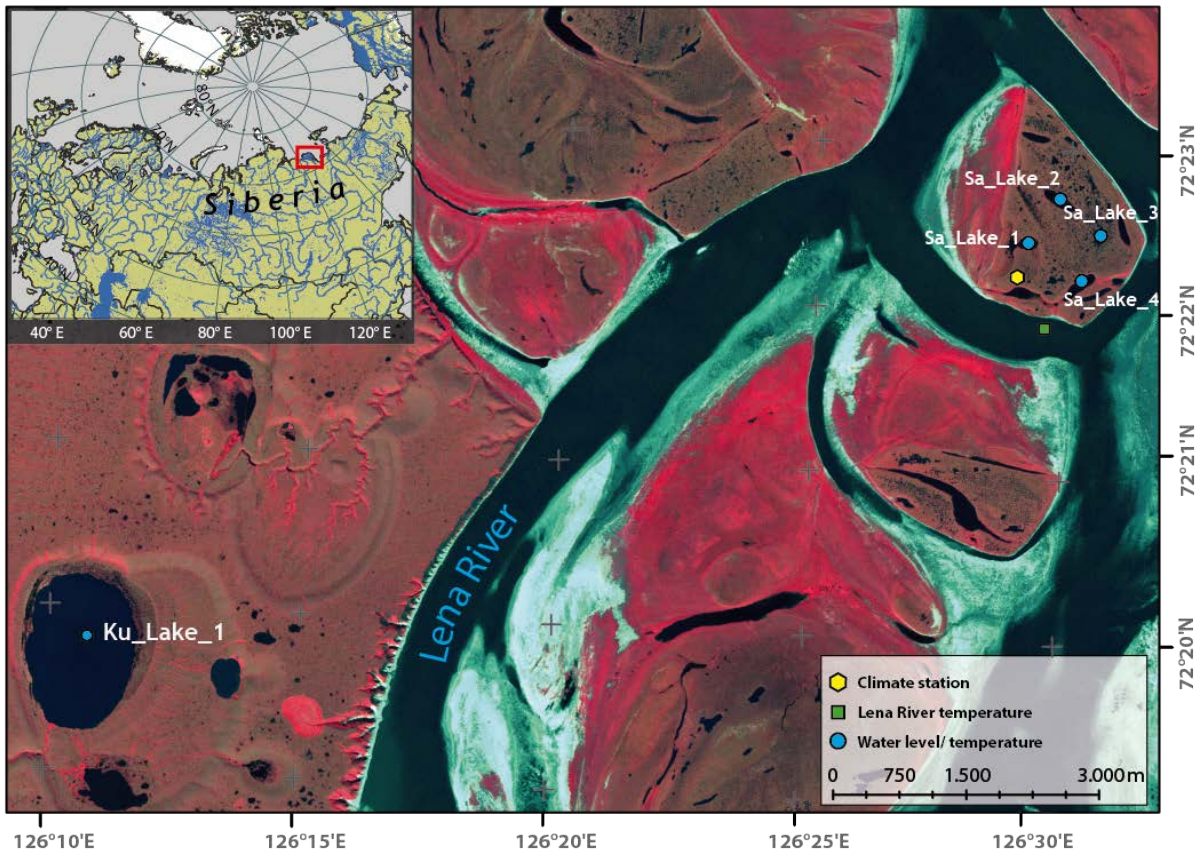
12 ^f mean value for ice-covered period (April – May 2014)

13 ^g mean value for the Lena River flood period (May – June 2014)

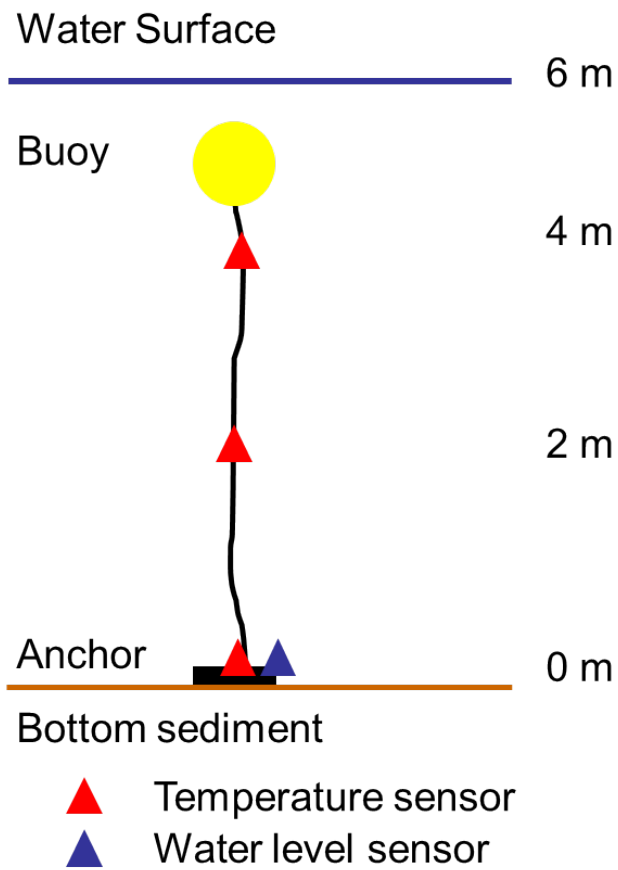
14 ^h mean value for summer period (July – August 2014)

15 ⁱ mean value for summer period (measured in July 2009)

16

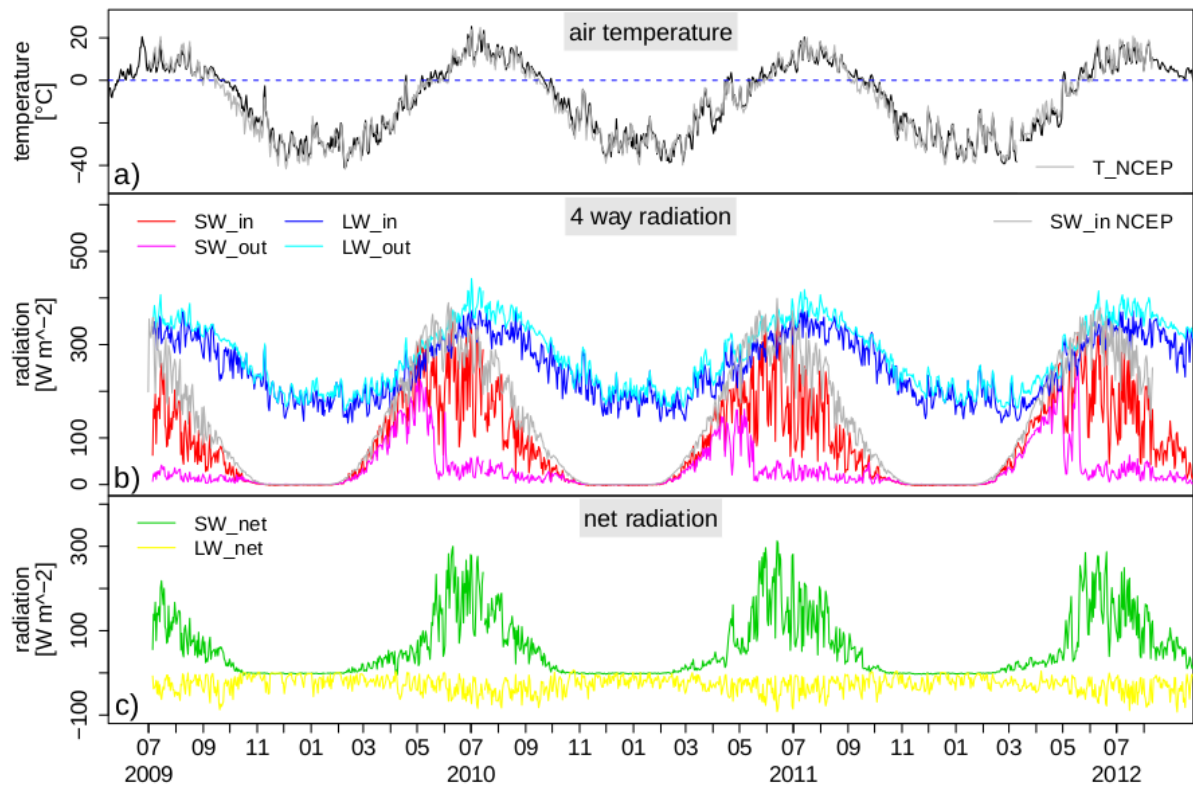


1
 2 Figure 1. Location of the study sites in the Lena River Delta of eastern Siberia; sites are
 3 within the zone of continuous permafrost on the islands of Kurungnakh (Ku_Lake_1), and
 4 Samoylov (Sa_Lakes_1-4). The inset map shows the location of the Lena River Delta in
 5 northern Eurasia and the distribution of lakes (Global lakes and wetland map; Lehner and
 6 Döll, 2004).



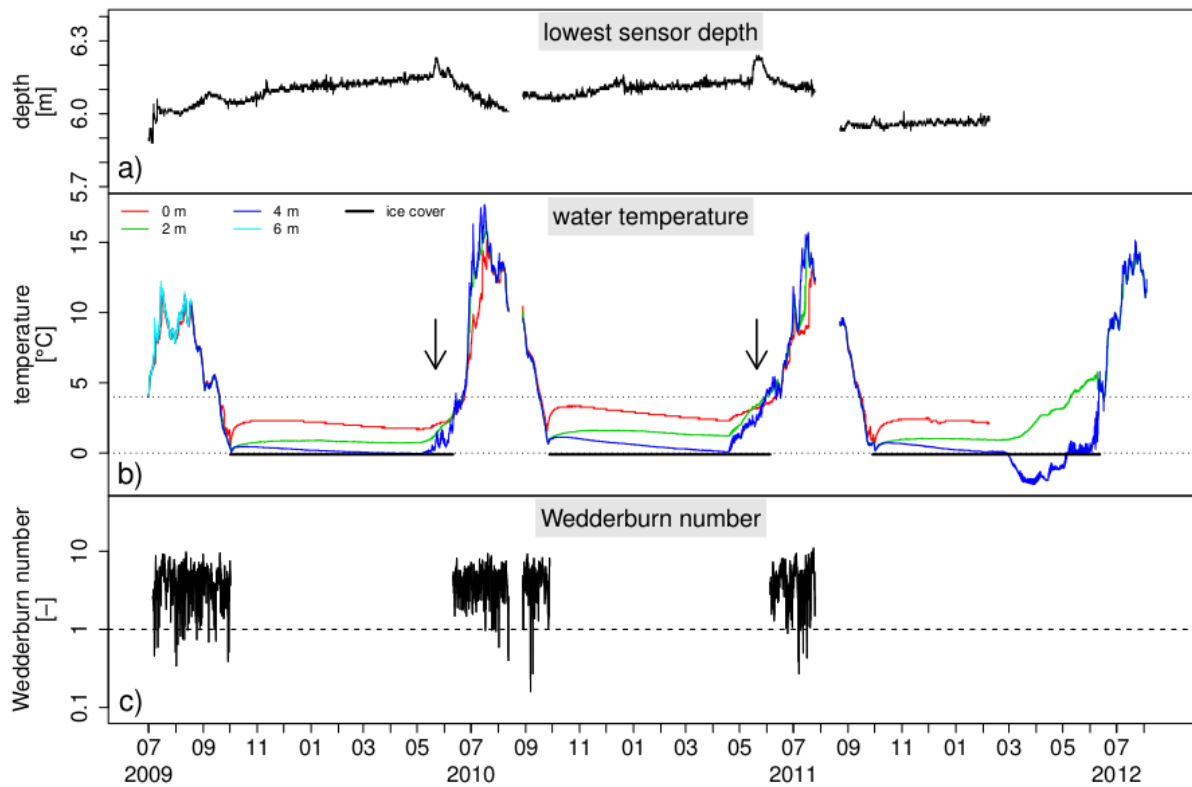
1

2 Figure 2. Schematic diagram showing the positions of sensors within the water column. To
 3 prevent freezing of the buoy within the ice cover (maximum 2 m thick), sensors were
 4 deployed 2 m below the water surface in most lakes. The water level sensor was located just
 5 above the bottom sensor, referred to in Figures 4 & 5 as the “lowest sensor depth”.



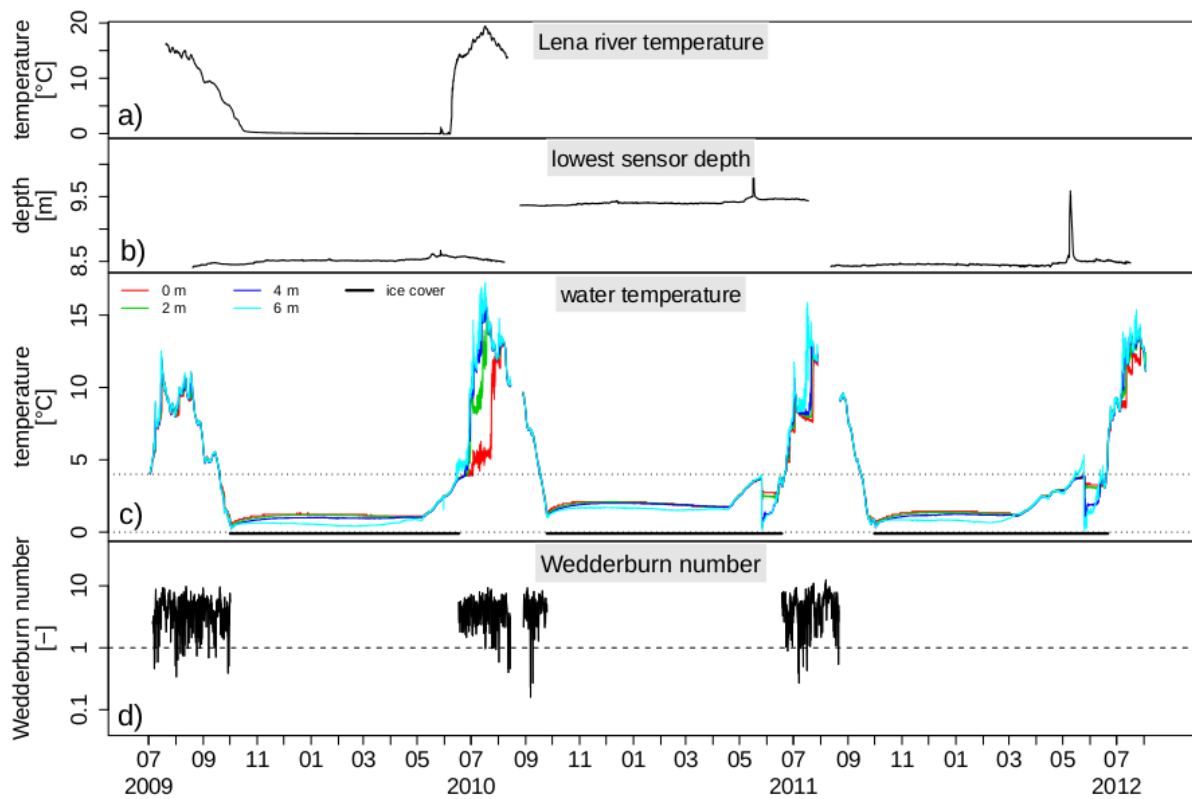
1

2 Figure 3. a) Mean daily air temperature at 2 m above ground level from Samoylov and NCEP;
 3 b) radiation balance (Samoylov) and shortwave incoming radiation (NCEP); c) net shortwave
 4 and longwave radiation (Samoylov) and radiation balance measured at the Samoylov climate
 5 station July 2009 - August 2012.

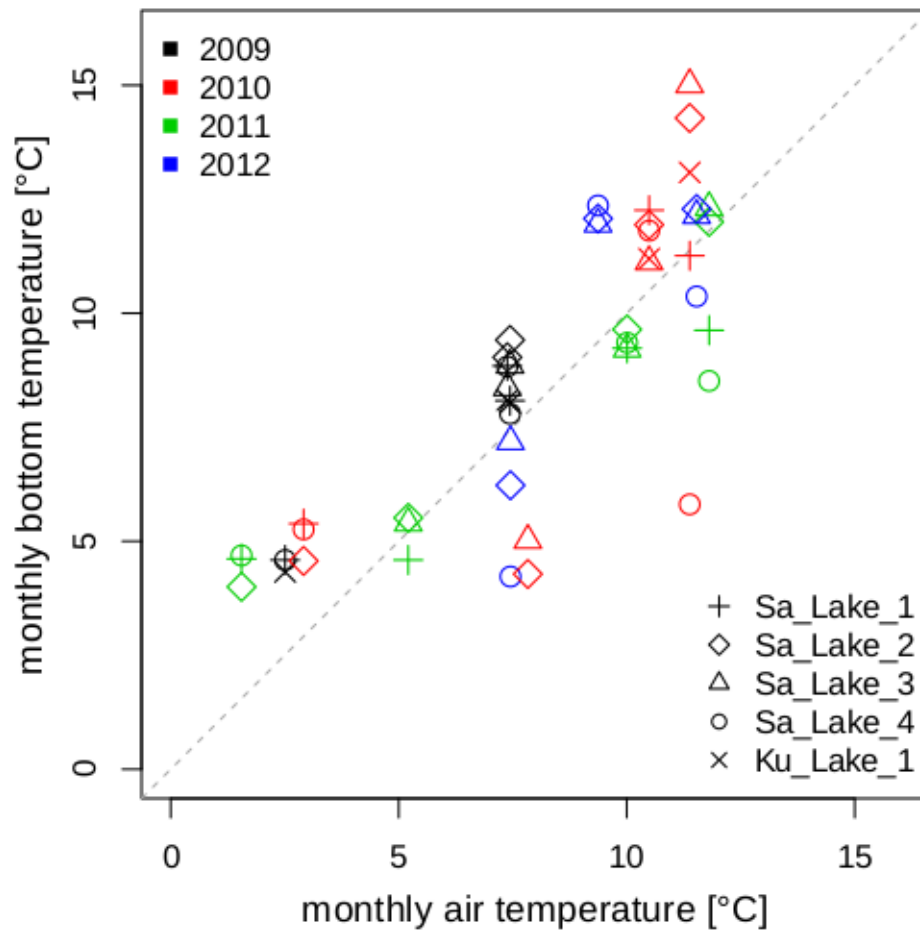


1

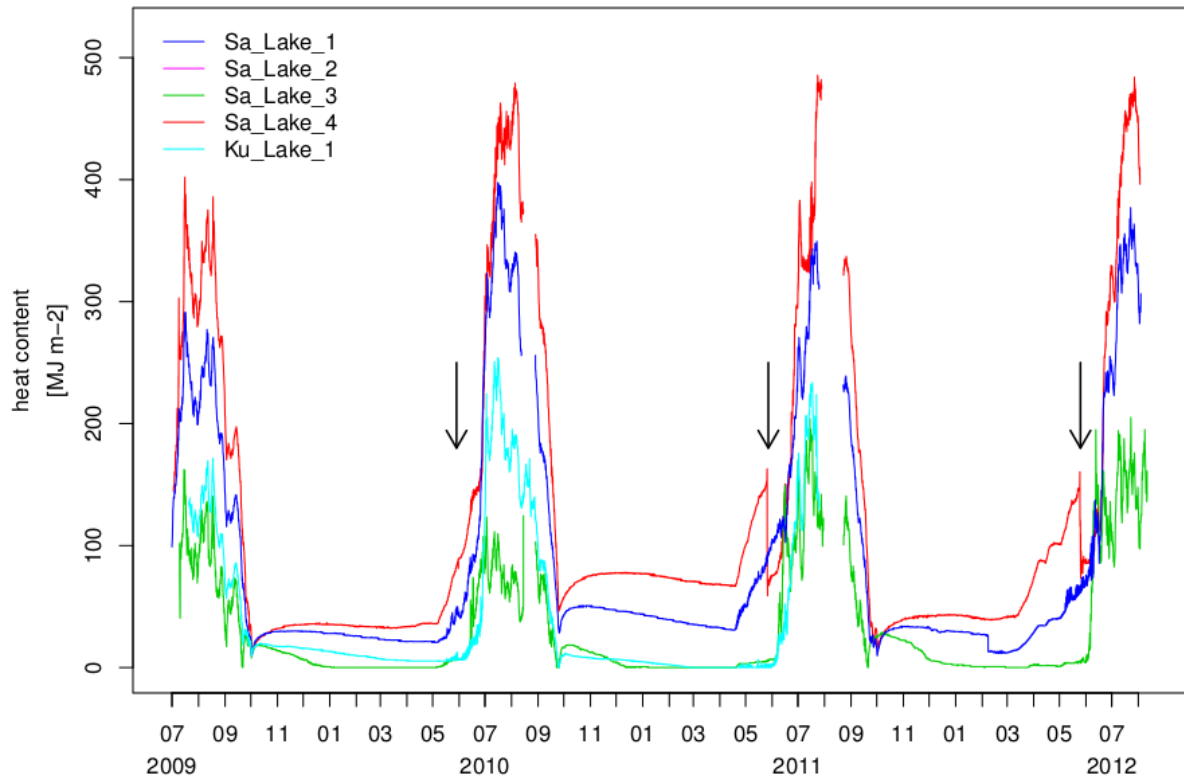
2 Figure 4. Hourly physical characteristics for Sa_Lake_1, July 2009 - August 2012. a) depth of
 3 bottom lake sensor as an indicator of water level changes; b) water temperatures and ice cover
 4 duration; c) Wedderburn number (dimensionless), calculated for the ice free period only.
 5 Arrows indicate the timing of the lake's seasonal flooding by Lena river water.



1
 2 Figure 5. a) Hourly temperatures for the Lena River from July 2009 to July 2010, and for
 3 Sa_Lake_4 (July 2009-August 2012): b) depth of bottom sensor as indicator for water level
 4 changes: sharp increase in depth during May 2011 and 2012 indicates flooding with Lena
 5 River water; c) water temperatures and ice cover duration (estimated from lake water
 6 temperatures); d) Wedderburn number (dimensionless) calculated for the ice-free period.
 7 Arrows indicate the timing of the lake's seasonal flooding by Lena river water.



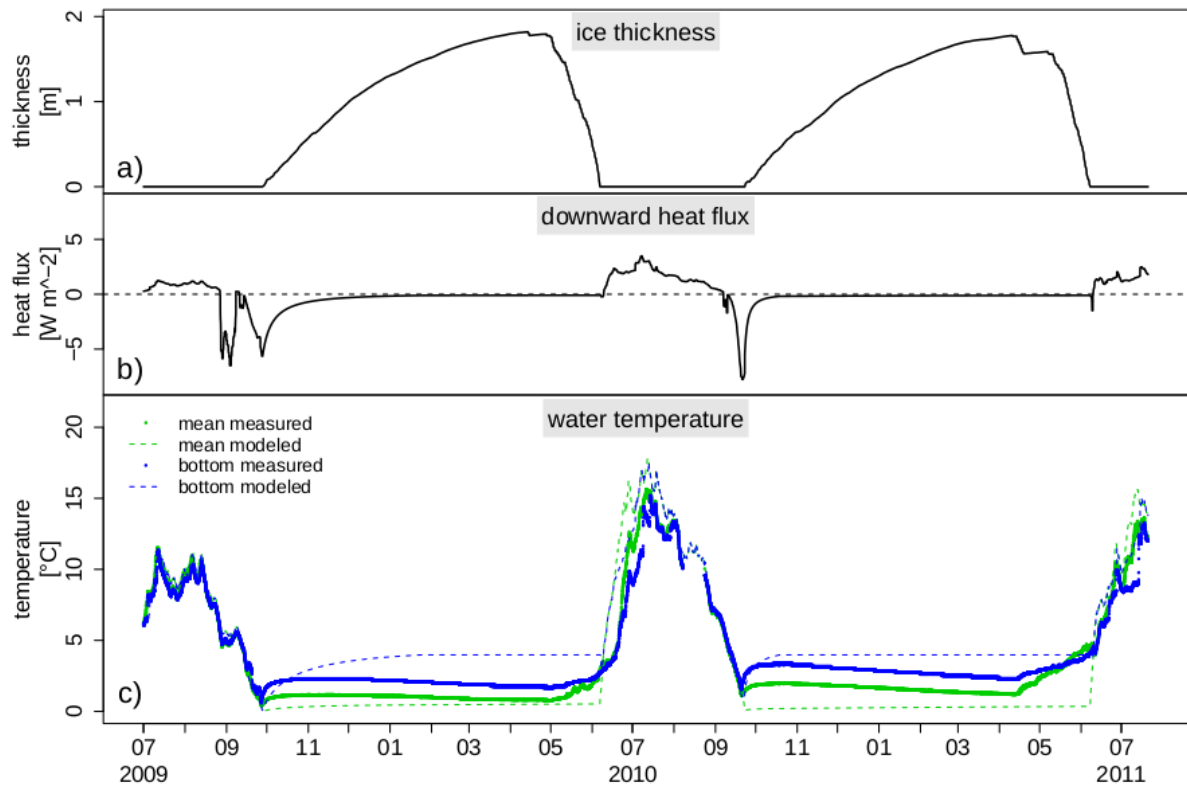
1
 2 Figure 6. Relationship between mean monthly lake bottom temperatures for all five lakes
 3 during the ice free period and the corresponding mean monthly air temperatures, from July
 4 2009 to August 2012. Data are also provided in the supplementary material of this paper.



1

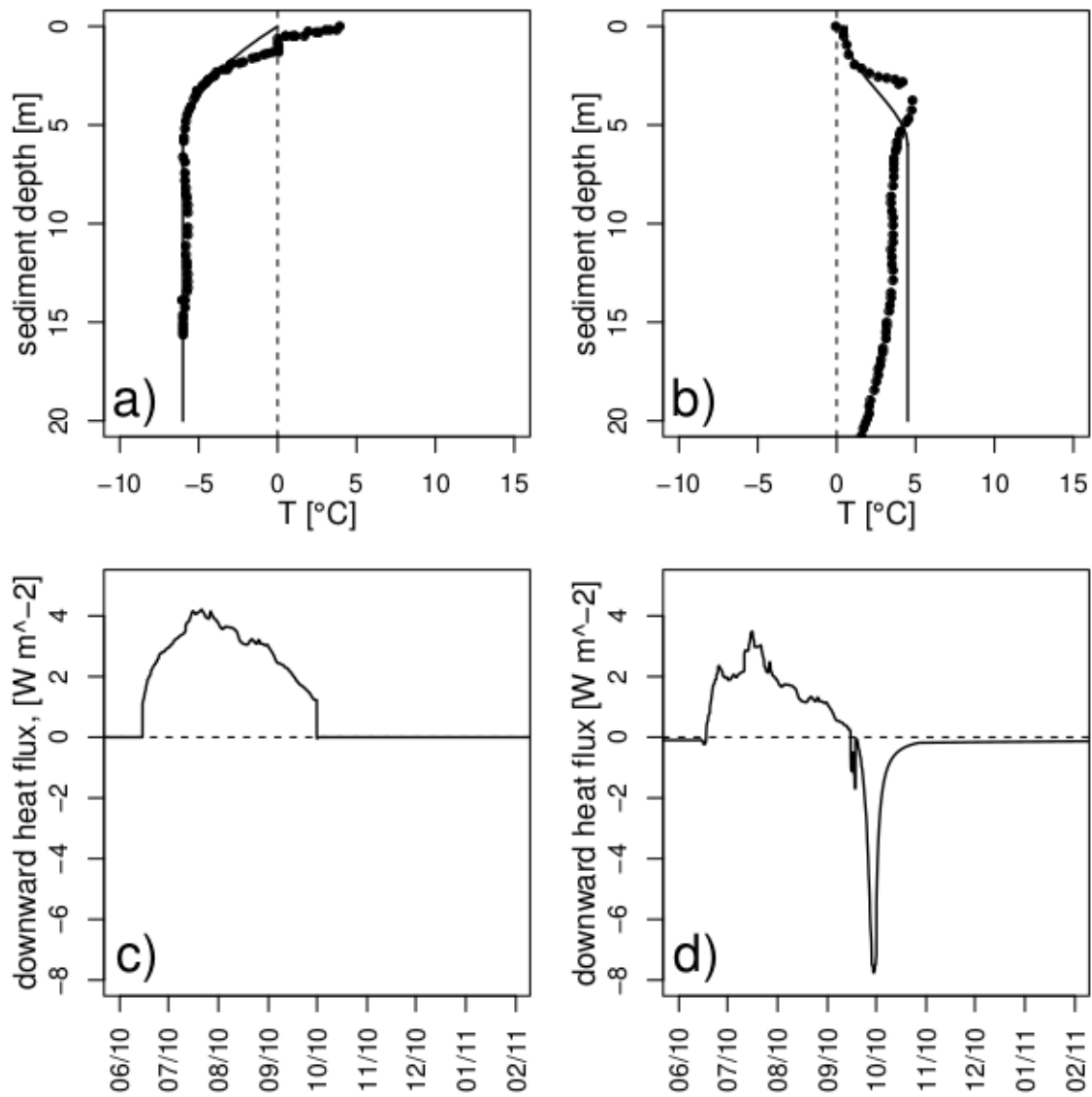
2 Figure 7. Sensible heat content (calculated using Equation 1) for the five lakes, from July
 3 2009 to August 2012. Arrows indicate the timing of the lake's seasonal flooding by Lena river
 4 water.

5

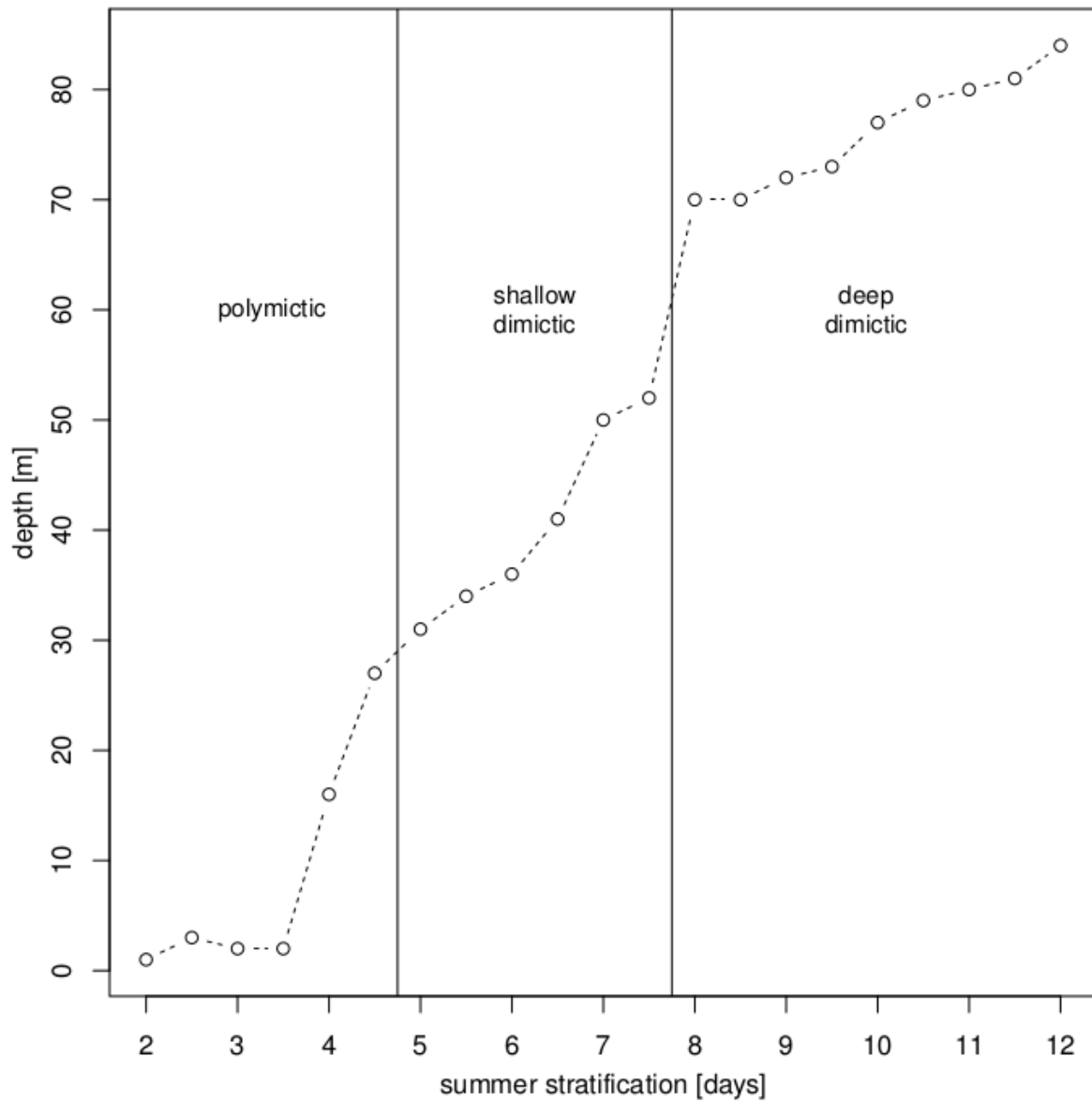


1

2 Figure 8. Modeled and measured hourly characteristics for Sa_Lake_1 from August 2009 to
 3 August 2011. a) Modeled ice thickness; b) modeled vertical heat flux at the water-sediment
 4 boundary: negative fluxes indicate fluxes from the sediment into the water column - a running
 5 median filter was used to remove spikes; c) measured (continuous line) and modeled (dashed
 6 lines) lake-bottom and mean water temperatures.

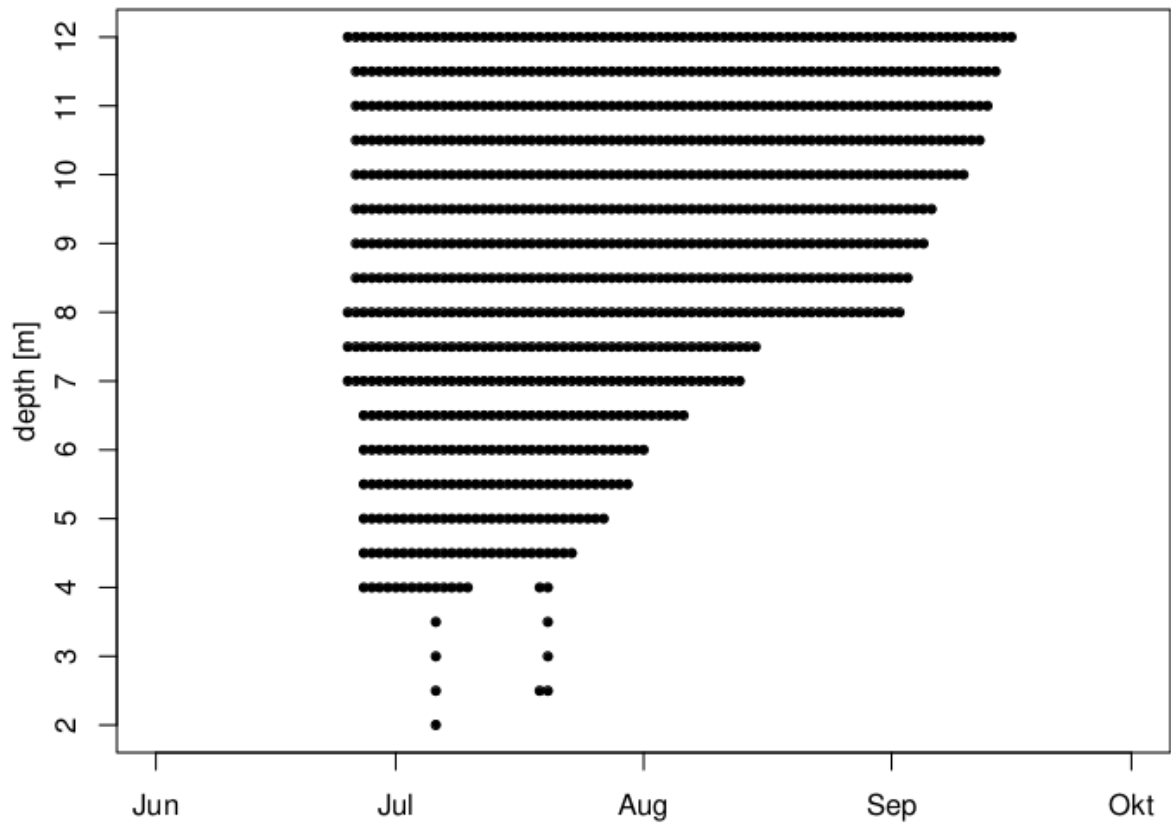


1
 2 Figure 9. a & b) Measured temperature profiles (squares) beneath two lakes (with a) 1 m
 3 water depth, and b) 5 m water depth) on the Bykovsky Peninsula, in the south-eastern part of
 4 the Lena River Delta (Grigoriev, 1993). Temperatures were measured between 9 and 11 June
 5 1984. Modeled sediment temperature profiles (continuous line) are for 10 June 2010 using
 6 model parameters described in the Methods section. c & d) Modeled daily vertical heat flux at
 7 the water-sediment boundary for c) the shallow lake, and d) the deep lake, 2010-2011.



1

2 Figure 10. Total number of days with summer stratification in lakes of varying depths
 3 modeled with FLake driven by the meteorological data from the Samoylov observatory
 4 station for 2010. Existence of stratification was determined by the criterion $(T_s - T_b) > 0.5^\circ\text{C}$,
 5 where T_s and T_b are the modeled temperatures at lake surface and lake bottom, respectively.

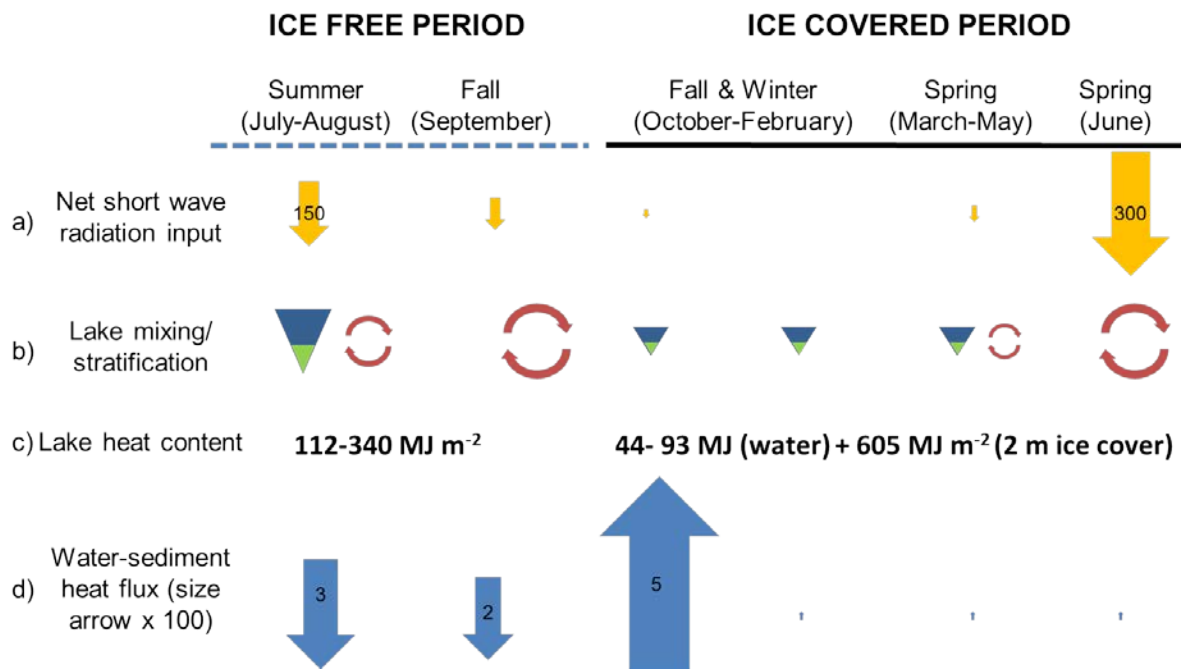


1

2

3 Figure 11. Summer stratification duration in lakes of varying depth (see Fig. 10 for
 4 definitions).

5

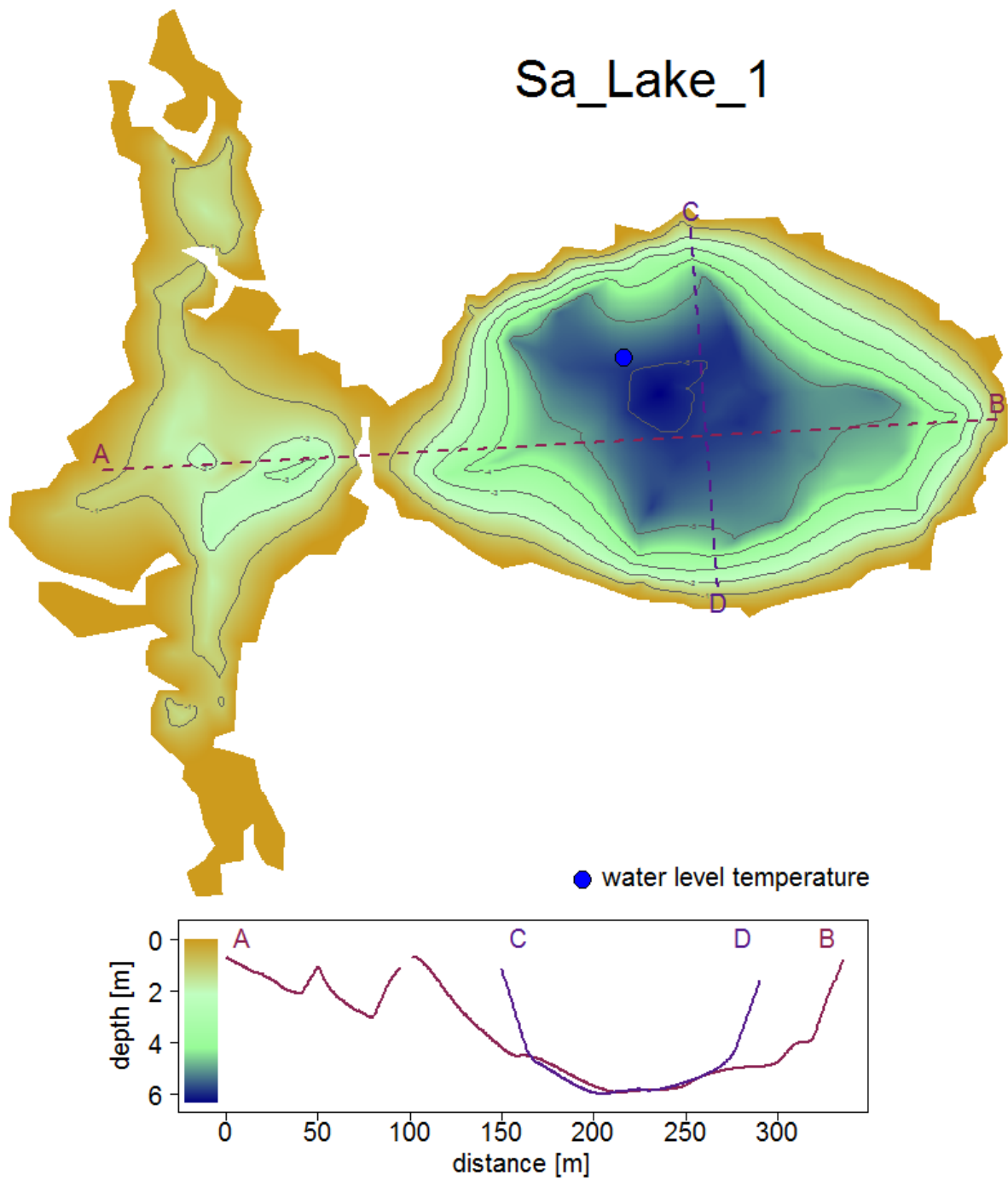


1
2 Figure 12. Summary of thermal processes in thermokarst lakes over a one year cycle. a) Net
3 short wave radiation input (measured at the climate station on Samoylov); b) dominant in-lake
4 processes (mixing and stratification) - size of symbol reflects intensity of process; c) lake heat
5 content (divided into summer and winter lake heat content according to Wetzel, 2001); d)
6 average heat fluxes across the lake's water-sediment boundary: downward arrows denote heat
7 flux into the sediment and upward arrows flux out of the sediment into the water column. The
8 size of the arrows and their numbers indicate the relative magnitudes of the fluxes [W m⁻²].
9 Note that the sizes of arrows representing bottom heat fluxes have been enlarged by a factor
10 of 100 due the small magnitude of the fluxes.

11
12

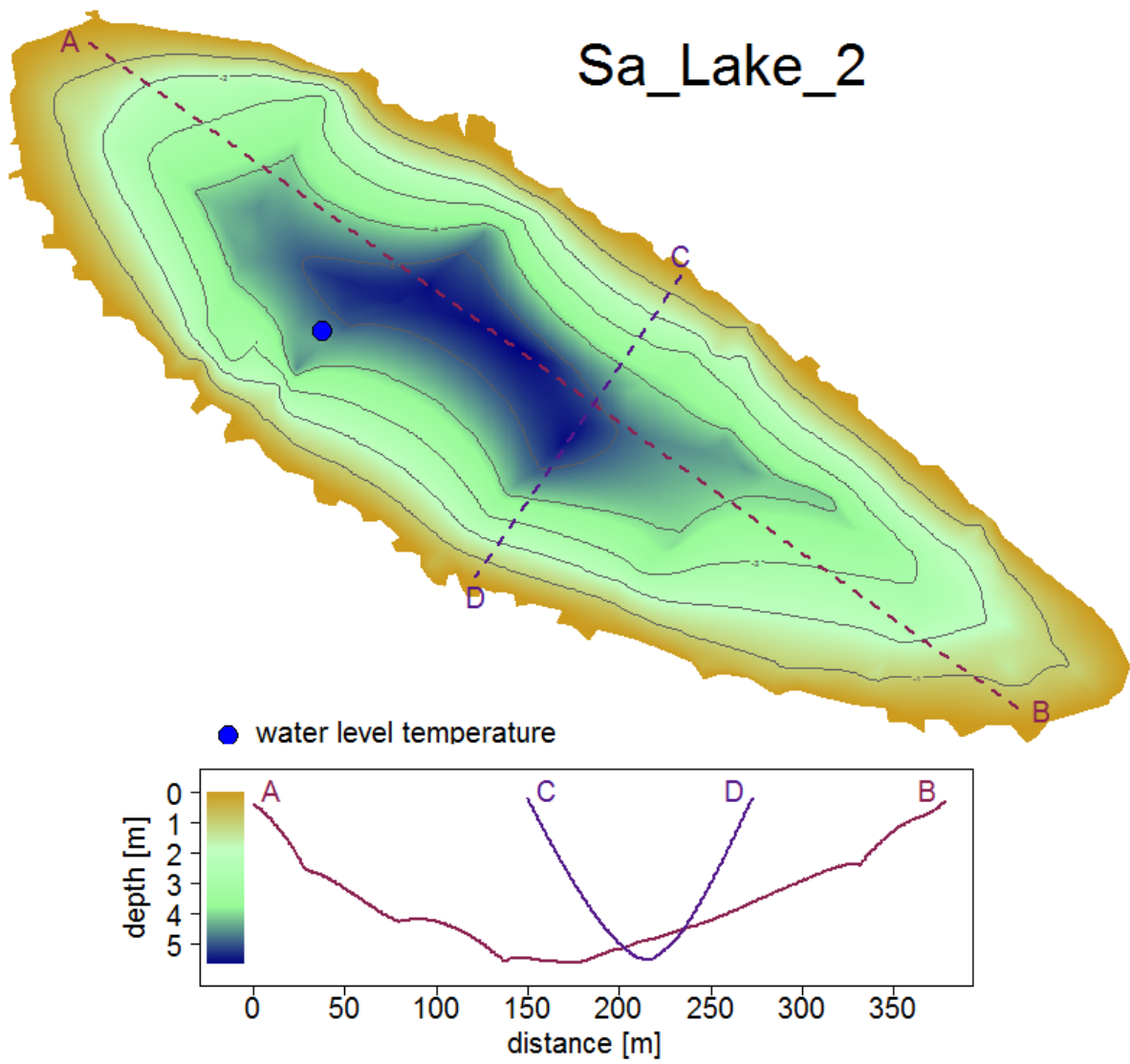
1 **Appendix A: Morphometry of lakes, hourly lake temperatures and lowest sensor depths**
2 **data**

3 The topographic slope on the polygonal tundra (first terrace) is very low ($< 5^\circ$). Aerial images
4 of Sa_Lake_2 and Sa_Lake_3 show submerged polygons beneath the water surface,
5 indicating that these lakes are likely to have been formed by the thawing of ground ice and ice
6 wedges and the subsequent merging of polygonal ponds. The shorelines adjacent to shallow
7 parts of these younger thermokarst lakes (with depths of 0-3 m) are very irregular and feature
8 protrusions of different shapes and sizes (Figures A1-A4). Where deeper sections (> 3 m)
9 occur close to the shore, the shorelines are smooth and the lakes tend to have an oval shape.
10 The profiles of thermokarst lakes tend to be V-shaped rather than flat-bottomed and the
11 thermokarst lakes investigated were up to 6.4 m deep. The deepest lake on this island, with up
12 to 11.6 m water depth, is Sa_Lake_4. It has an elongated shape and is one of three
13 interconnected lakes that occur in an abandoned channel of the Lena River ("oxbow" or
14 "perched" lakes; Figure A4). The largest monitored lake in this series of lakes was
15 Ku_Lake_1, located on sediments of the Pleistocene Ice Complex, which have high ice
16 content. This lake is the largest of three residual lakes located within an alas that is more than
17 20 m deep. This thermokarst basin evolved in two phases (Morgenstern et al., 2013). In the
18 first phase the original large lake covered the entire basin. It drained abruptly through a
19 thermos-erosional valley at about 5.7 ka BP, leaving the > 20 m deep alas with residual lakes.
20 This was then followed by thermokarst processes of varying intensity during the second phase
21 (5.7 ka BP to the present). This lake is an order of magnitude larger in surface area than the
22 other four thermokarst lakes investigated and, in contrast to those lakes on Samoylov Island,
23 has a regular oval shape, occurs within a basin with steep sides and has a smooth, flat
24 shoreline. The maximum water depth is about 3.6 m and the profile is flat-bottomed (Figure
25 A5).



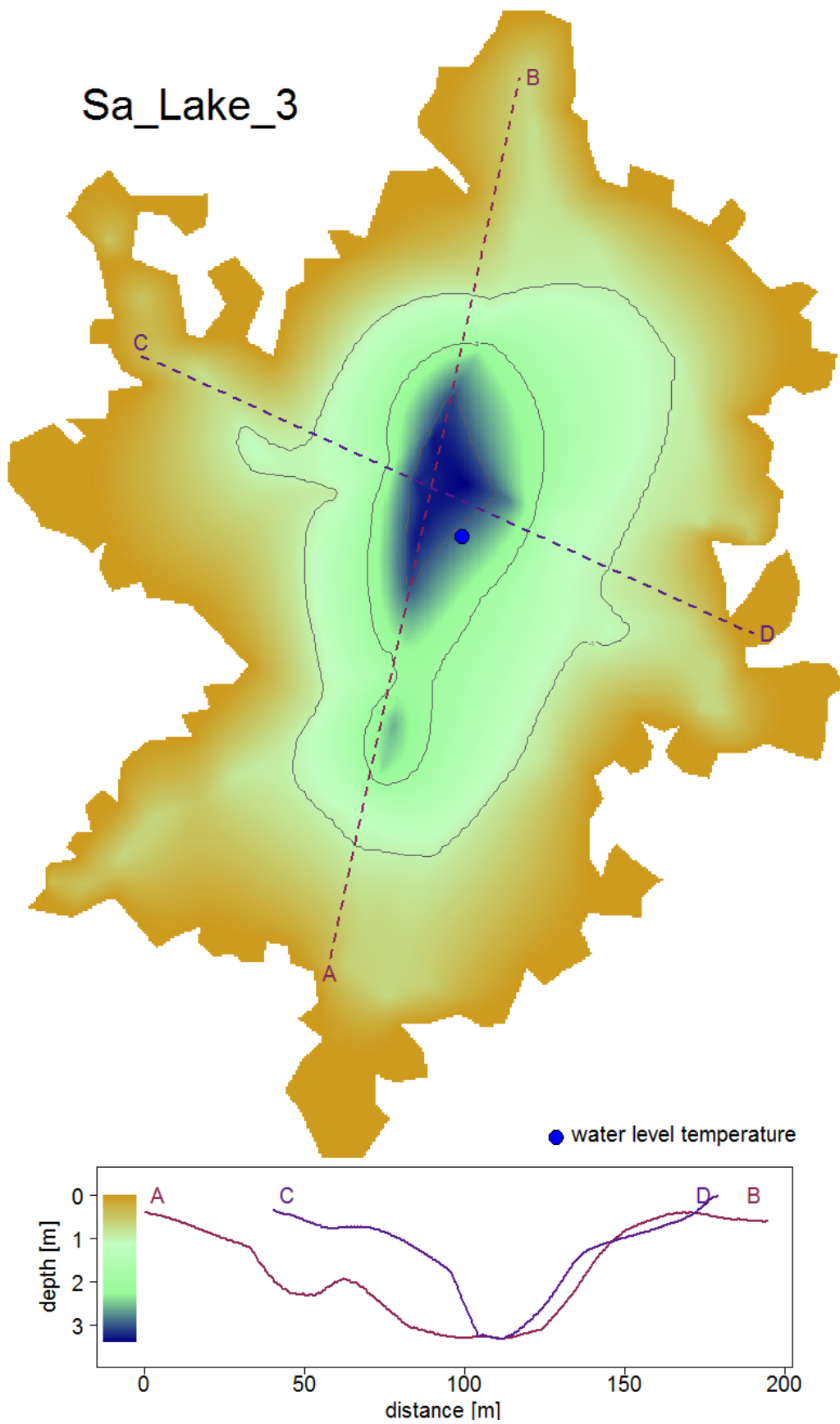
1

2 Figure A1. Bathymetry and cross sections of Sa_Lake_1 with location of sensors.



1

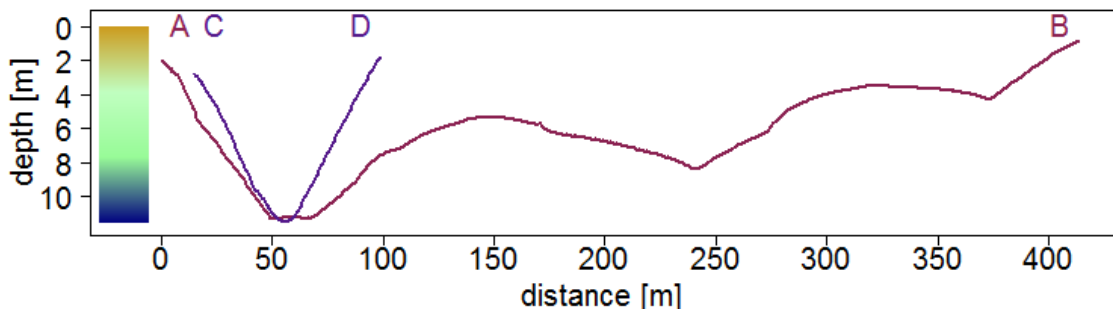
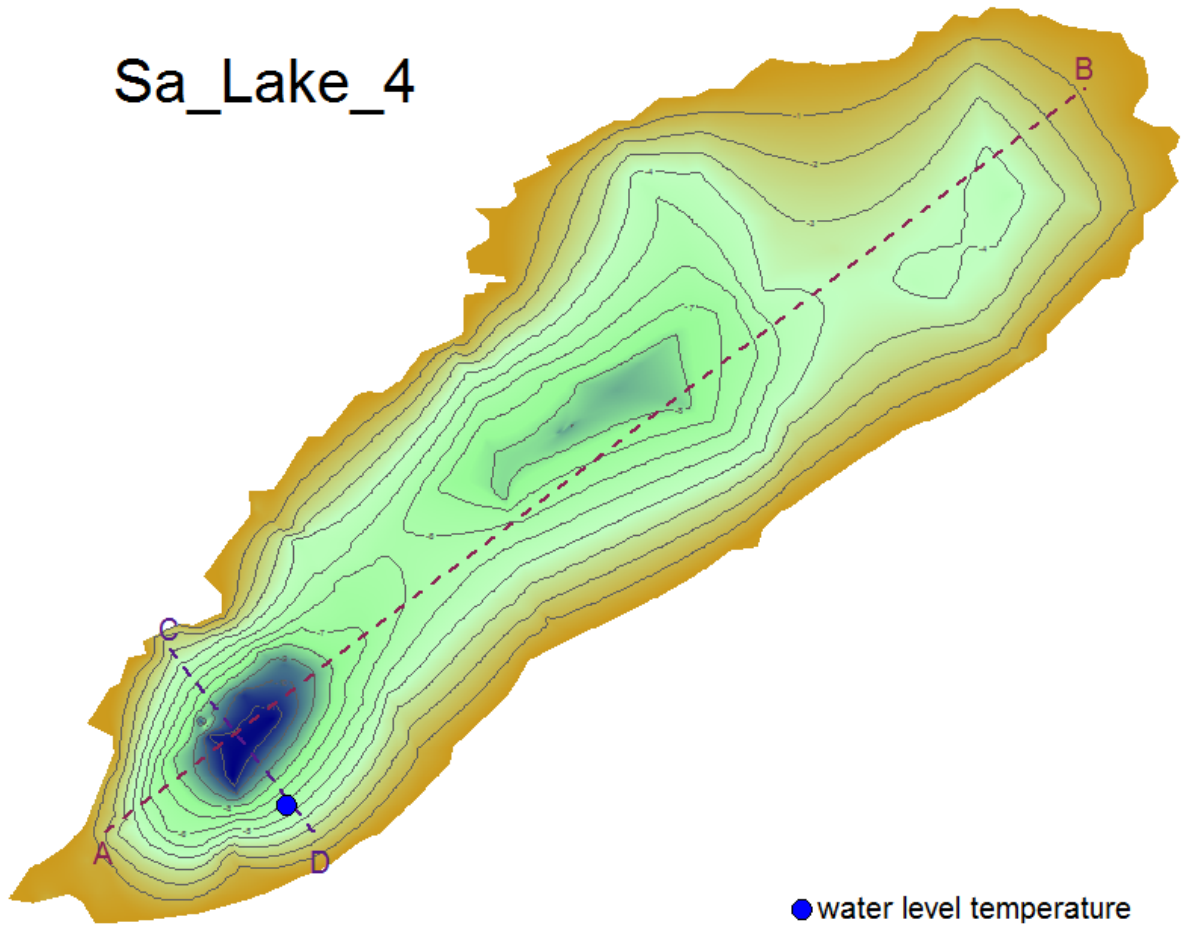
2 Figure A2. Bathymetry and cross sections of Sa_Lake_2 with location of sensors.



1

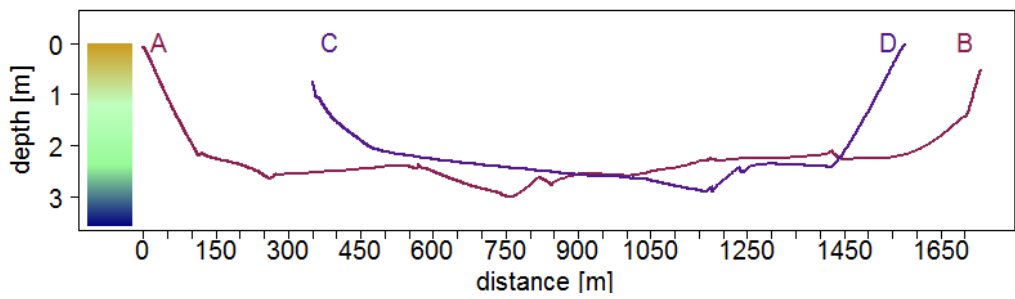
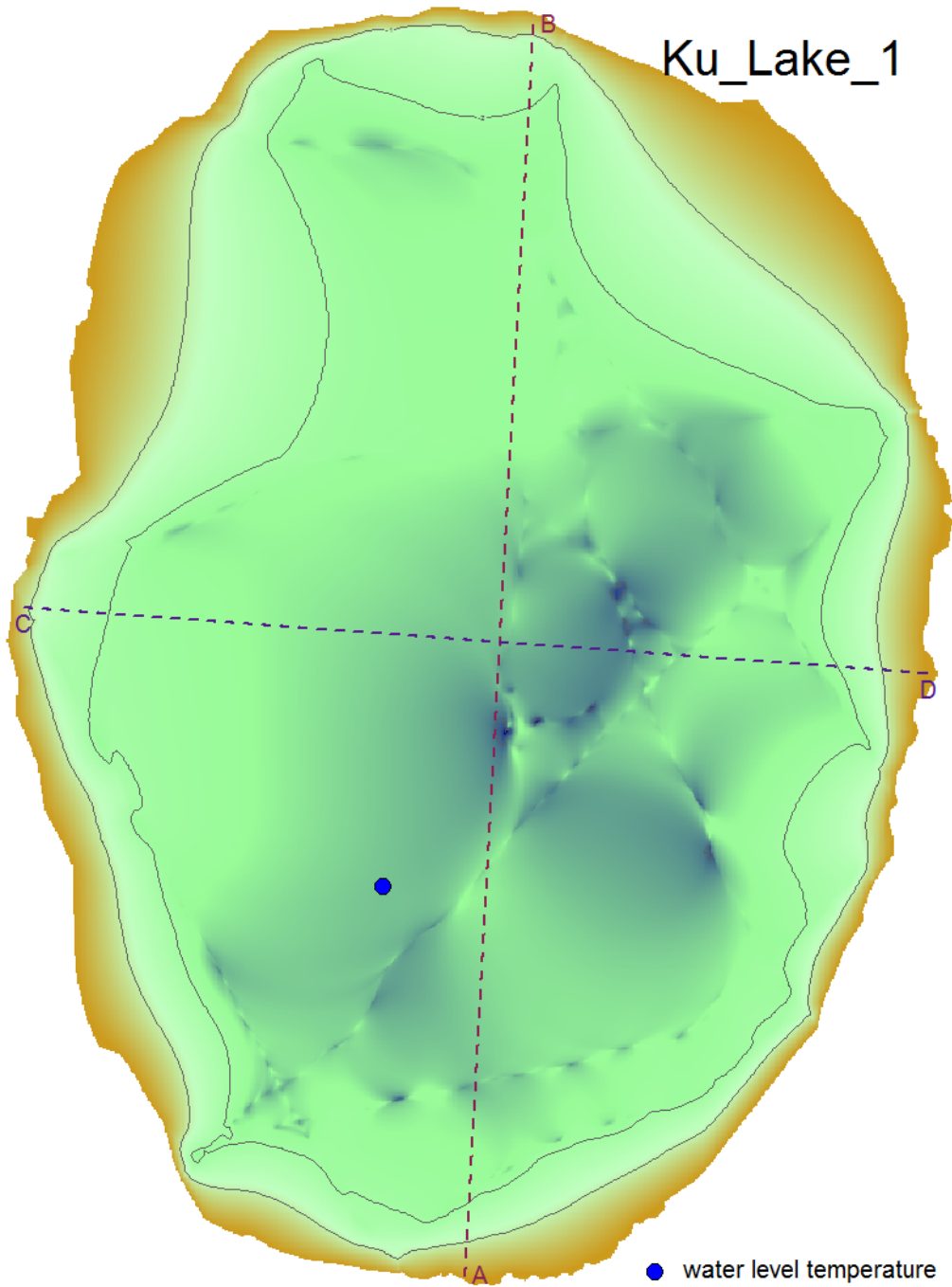
2 Figure A3. Bathymetry and cross sections of Sa_Lake_3 with location of sensors.

Sa_Lake_4



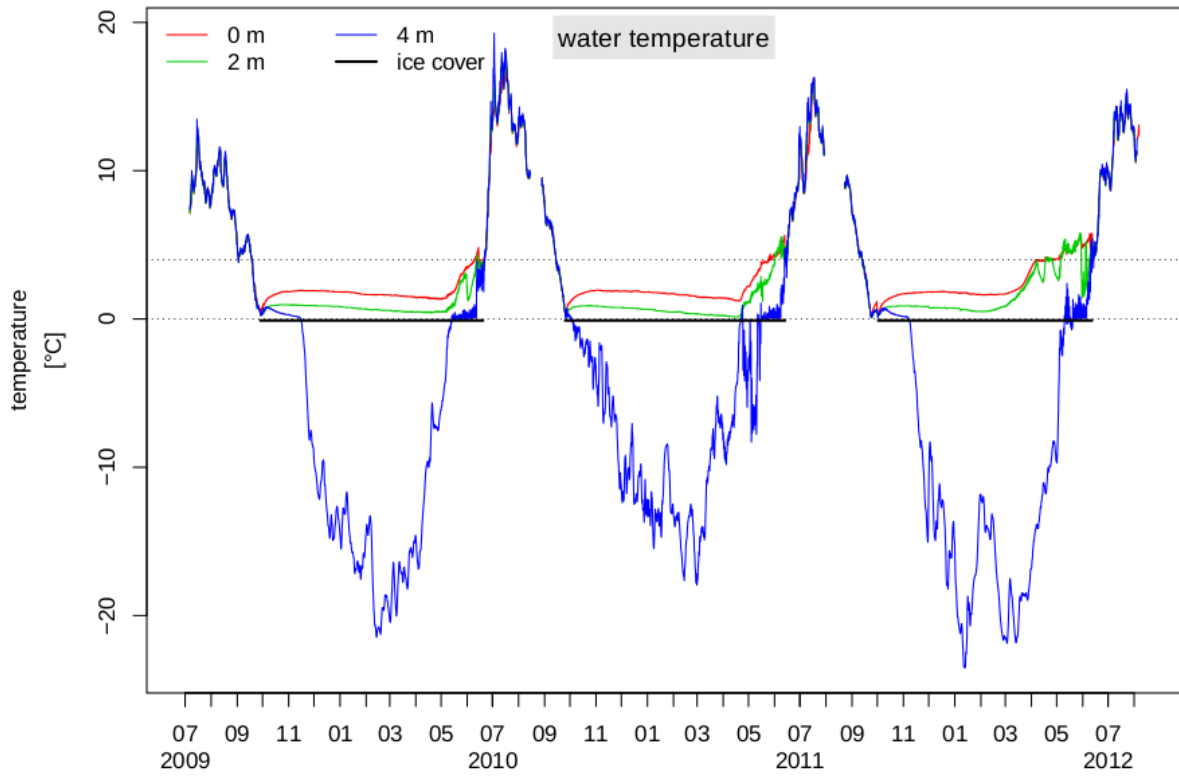
1

2 Figure A4. Bathymetry and cross sections of Sa_Lake_4 with location of sensors.



1

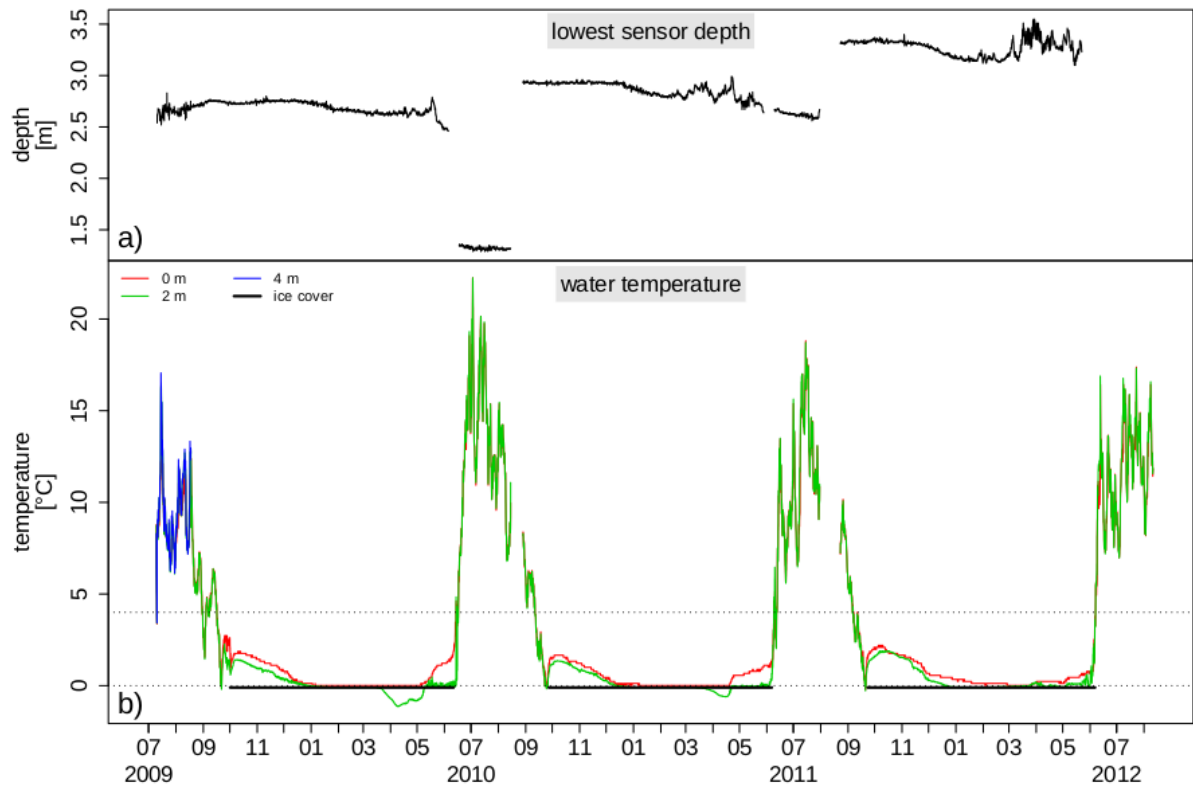
2 Figure A5. Bathymetry and cross sections of Ku_Lake_1. (Data from Morgenstern et al.,
 3 2011 and <http://doi.pangaea.de/10.1594/PANGAEA.848485>).



1

2 Figure A6. Hourly lake temperatures and lowest sensor depth (indicating water level changes)
 3 for Sa_Lake_2, from July 2009 to August 2012. Thick black lines indicate ice covered
 4 periods.

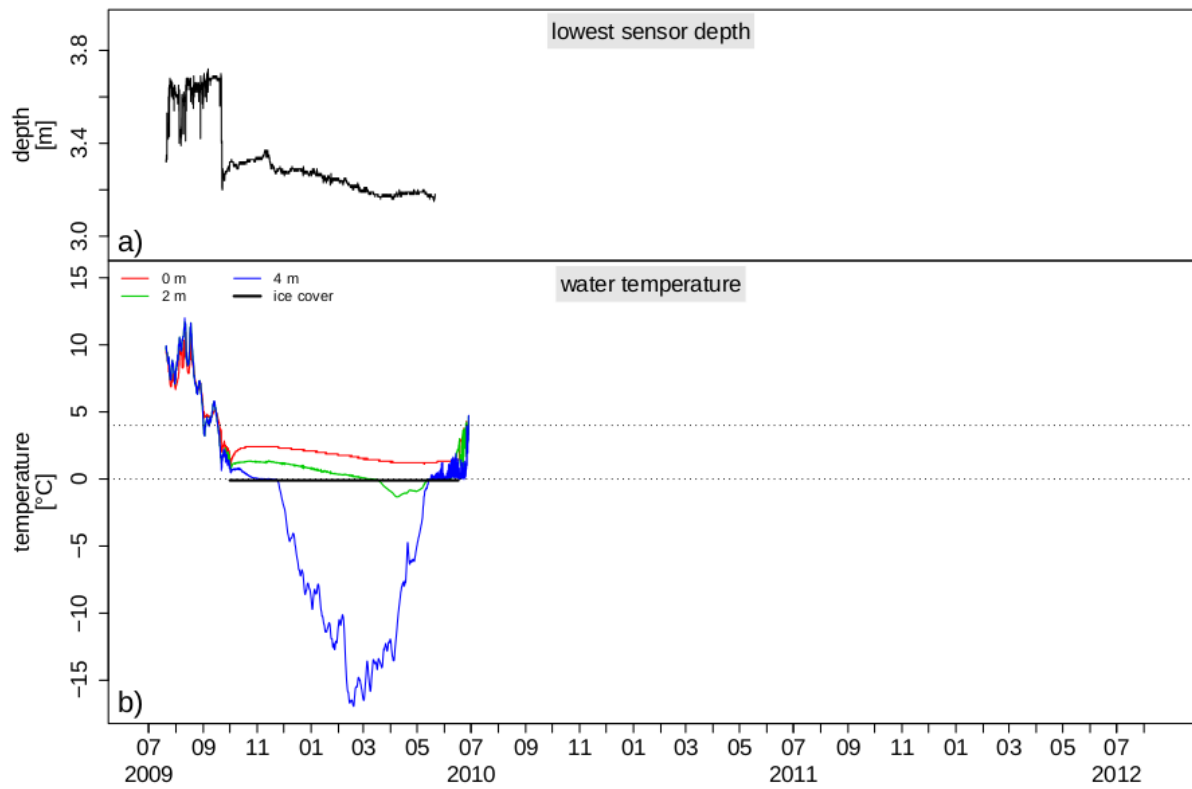
5



1

2 Figure A7. Hourly lake temperatures and lowest sensor depth (indicating water level changes)
 3 for Sa_Lake_3, from July 2009 to August 2012. Thick black lines indicate ice covered
 4 periods.

5



1

2 Figure A8. Hourly lake temperatures and lowest sensor depth (indicating water level changes)
 3 for Ku_Lake_1, from July 2009 to August 2010. Thick black lines indicate ice covered
 4 periods.

5

1

2 **Supplementary material: data and animations**

- 3 • Model data input (Samoylov); air temperature, air humidity, wind speed; radiation
4 components

5 Samoylov_2009_2012.dat

6

- 7 • Model validation data: hourly lake temperatures and sensor depth (lake water level)
8 data, where measured

9

10 Sa_Lake_1_2009_2012.dat

11 Sa_Lake_2_2009_2012.dat

12 Sa_Lake_3_2009_2012.dat

13 Sa_Lake_4_2009_2012.dat

14 Ku_Lake_1_2009_2010.dat

15 LenaRiver_2009_2010.dat

16

- 17 • Animation (movie) of temperatures in Sa_Lake_1 using daily average temperatures at
18 depth and interpolated between depths using cubic interpolation. Daily temperature
19 plots were added to produce the animation of temperatures

20 Sa_Lake_1_2010-daily-color-.2s.gif

21

- 22 • Summary table of mean monthly air and bottom lake temperatures:
23 meanlake_air_temp.txt

24

25